



# The computational cost of active information sampling before decision-making under uncertainty

Pierre Petitet <sup>1</sup>✉, Bahaaeddin Attaallah <sup>2</sup>, Sanjay G. Manohar <sup>1,2</sup> and Masud Husain <sup>1,2</sup>✉

**Humans often seek information to minimize the pervasive effect of uncertainty on decisions. Current theories explain how much knowledge people should gather before a decision, based on the cost–benefit structure of the problem at hand. Here, we demonstrate that this framework omits a crucial agent-related factor: the cognitive effort expended while collecting information. Using an active sampling model, we unveil a speed–efficiency trade-off whereby more informative samples take longer to find. Crucially, under sufficient time pressure, humans can break this trade-off, sampling both faster and more efficiently. Computational modelling demonstrates the existence of a cost of cognitive effort which, when incorporated into theoretical models, provides a better account of people’s behaviour and also relates to self-reported fatigue accumulated during active sampling. Thus, the way people seek knowledge to guide their decisions is shaped not only by task-related costs and benefits, but also crucially by the quantifiable computational costs incurred.**

Obtaining information is a crucial part of normal decision-making under uncertainty. For example, deciding where to go out for dinner requires building predictions about how good the food, atmosphere and service will be in nearby restaurants. Incorrect predictions can ultimately result in poor choices, leading to deviations from the intended outcome (for example, a bad dinner). Such disappointing experiences can be prevented, however, by spending time to gather information before making a decision, in order to reduce uncertainty and improve predictions. To do this, humans need to solve two key problems. First, they need to identify, in a complex, high-dimensional world, what constitutes potentially useful information, and devise a strategy to extract it efficiently. For instance, should they read online customer reviews, ask a friend or check a guidebook? Second, they must set a stopping policy that determines when to stop gathering information and use the knowledge accumulated to guide their final decision.

Current accounts of active information gathering<sup>1–6</sup> are grounded in neuroeconomic theories of decision-making<sup>7–11</sup>. According to this perspective, people behave to maximize the expected utility of their final decision (that is, how rewarding the outcome of their choice is likely to be). A discrete piece of information (sample) is worth acquiring in this framework only if the instrumental benefit it provides outweighs the cost of obtaining it. This instrumental benefit is the increase in expected utility that results from making the final decision with the information, compared to without it. Such an approach has proven useful in understanding why people seek more knowledge when sampling is cheap, errors are strongly penalized or the information content of individual samples is low<sup>1,5,6,12–17</sup>. In other words, it provides a useful conceptual framework for understanding how stopping policies respond to changes in the cost–benefit structure of the task environment.

Previous investigations of cognitive information sampling have largely focused on characterizing such stopping policies. They have used simple models in which resources (for example, monetary credits) could solely be used towards acquiring more, but crucially not better, samples<sup>1,5,13,18</sup>. However, such an approach neglects the fact that, in day-to-day life, not all potential samples are equally

informative. Instead, a well-chosen piece of information may have the potential to strongly resolve uncertainty, while others may be irrelevant. It is therefore important to determine which information to acquire, in addition to how much, before making a decision. Crucially, the process of identifying the best sample to collect may require cognitive effort as well as time, adding to a computational cost that is currently not accounted for by theoretical models of active information sampling<sup>19,20</sup>.

Two factors that theoretically might contribute to this computational cost are worth considering in more detail. First, identifying samples that are more informative potentially takes longer and thus carries an opportunity cost<sup>21,22</sup>. In the restaurant example, asking a friend may provide more useful information than consulting a guidebook, but we risk not obtaining that information before dinner if it requires texting, then awaiting a response. Here, the opportunity cost is the potentially useful information missed because of the decision deadline. Numerically, it is therefore a function of the agent’s sampling strategy (speed and efficiency), as well as the task’s cost–benefit and temporal structure. The second factor is a potential cognitive effort cost<sup>23,24</sup>, which arises from mechanisms that enhance the amount of information gathered per unit of time<sup>25</sup> (for example, increasing the rate at which candidate samples are assessed, inhibiting unhelpful automatic or habitual responses or allocating more attentional resources to the search for knowledge). For example, if we decide to phone our friend, we might obtain more information by turning the conversation towards the features of a restaurant that interest us most and paying close attention to the responses. The cognitive effort expended in honing in on the most valuable information might lead to better decisions but also incur a cost in terms of neural resources and/or energy consumption.

We hypothesized that if people discount the computational cost expanded from information benefits, active sampling for information before decision-making should be more flexible than is currently assumed. Testing this empirically requires experimental features that are missing from existing paradigms<sup>1,13,18,26,27</sup>: (1) some candidate samples should be more informative than others; and (2) it should be non-trivial to find them. Here, we designed a more

<sup>1</sup>Department of Experimental Psychology, University of Oxford, Oxford, UK. <sup>2</sup>Nuffield Department of Clinical Neurosciences, University of Oxford, Oxford, UK. ✉e-mail: [pierre.petitet@gmail.com](mailto:pierre.petitet@gmail.com); [masud.husain@ndcn.ox.ac.uk](mailto:masud.husain@ndcn.ox.ac.uk)

complex, active information-sampling task that incorporates these key features. In our paradigm, people search spatially for information, by touching screen areas, before committing to an answer. Importantly, some sample locations give more information than others, but finding them is not straightforward.

Using this model, we demonstrate, over five separate experiments, that information sampling before decision-making is extremely flexible and adapts to contextual constraints. People are able to increase the rate at which they accumulate knowledge, either by acquiring data faster or by slowing down to select better observations at each step. Thus, the results demonstrate a speed–efficiency trade-off whereby more informative samples take longer to find. But, crucially, when under sufficient time pressure (when there is a substantial opportunity cost), humans are capable of breaking this trade-off, sampling both faster and more efficiently. To account for such flexibility, we posit a cognitive control mechanism that arbitrates how quickly and efficiently people sample information. In our model of cost–benefit evaluation, both speed and efficiency are treated as costly, incurring a cognitive effort cost for the individual. Furthermore, this effort cost relates to subjective self-reported fatigue accumulated during active sampling. Taken together, these findings show that incorporating a computational (cognitive) cost into classical models of active information sampling provides a better account of human behaviour before decisions are made under uncertainty.

## Results

**Active information-sampling model.** A schematic of the model, framed as a game called Circle Quest, is depicted in Fig. 1a. The goal was to maximize earnings in the form of credits. Players searched for information about the location of a hidden circle (radius = 130 pixels) by tapping a touchscreen with their index finger. If they touched inside the hidden circle, a purple dot appeared; otherwise, if they touched outside the hidden circle, a white dot appeared. These dots, denoting the results of sampling at various locations, stayed on the screen throughout the information-sampling phase and until the end of the trial in order to limit memory load. Participants started each trial with a certain number of credits (starting credit,  $R_0$ ), which decreased by a fixed amount every time they acquired a sample (sampling cost,  $\eta_s$ ). During the time allocated to sampling ( $t_{\max}$ ), they were free to acquire as many samples as judged necessary, at the rate they preferred, anywhere in the search space. Once this time elapsed, individuals were asked to place a blue disk where they thought the hidden circle was located. This response was subsequently rewarded according to the following scoring function:  $R_0 - (s \times \eta_s) - (e \times \eta_e)$ , where  $s$  is the number of samples acquired,  $e$  is the placement error (in pixels) and  $\eta_e$  is the error cost (linear cost, in credits per pixel). Thus, performing well in this task required minimizing uncertainty to avoid large error penalties while also minimizing sampling-related losses.

**Quantifying uncertainty with the expected error.** In this model, uncertainty pertains to the location uncertainty of the hidden circle in the search space. It was quantified objectively as the expected error (in pixels), that is, the error an ideal observer is most likely to obtain by placing the blue circle at the best possible location given the observations on the screen (Fig. 1b; details in Supplementary Methods). This formalism is more suited than the entropy of the posterior belief (another measure of uncertainty quantifying the size of the solution space on a log scale) because it has direct instrumental implications in the game ( $EV = R - (\eta_e \times EE)$ , where  $EV$  is the rational expected value and  $\eta_e \times EE$  is the expected error penalty). Because the expected error is a rather abstract dimension that may be difficult to intuit, we first asked, using a simplified counterpart of the game, whether participants were able to manipulate this variable within a decision-making problem.

In experiment 1a, eight samples were presented on the screen (four white and four purple) and individuals ( $n = 48$ ; mean age = 24.52 years; s.d. = 3.75 years; Extended Data Fig. 1) simply had to rate, on a visual analogue scale, how well they thought they could localize the hidden circle (Fig. 2a; see Methods). In this task, there was no active sampling; instead, participants simply made judgements on a single snapshot, which provided them with information. Uncertainty (the expected error) was manipulated experimentally by varying the geometrical distribution of the samples. On a trial-by-trial basis, directly after their confidence rating, the number of available credits appeared (40, 70, 100 or 125 credits) and individuals had to indicate whether or not they would accept the offer to place the blue disk for this combination of reward and uncertainty. To incentivize authentic choices, participants were instructed that at the end of the experiment they would have to play (that is, place the blue circle and win credits according to their performance) for a fixed number of trials, selected from the preferences they expressed.

Uncertainty ratings were calculated by sign flipping and  $z$ -scoring confidence ratings for each individual. The objective uncertainty (expected error) showed a significant linear relationship with these subjective ratings (linear mixed model (LMM); standardized  $\beta = 0.80$ ; 95% confidence interval (CI) = (0.76, 0.83);  $t_{(8062)} = 49.89$ ;  $P < 0.001$ ; Supplementary Table 1 and Fig. 2b), suggesting that participants were reporting an internal variable that resembled the expected error. This metric in fact provided a good predictive estimate of actual placement errors (Supplementary Fig. 1). Furthermore, as demonstrated by logistic linear modelling of accept–reject decisions, individuals correctly weighed the expected error against reward in order to decide whether or not to place the blue circle (mixed-effects logistic regression; main effect of expected error: standardized  $\beta = -2.53$ ; 95% CI = (-2.80, -2.27);  $t_{(8060)} = -8.57$ ;  $P < 0.001$ ; main effect of reward: standardized  $\beta = 1.87$ ; 95% CI = (1.49, 2.26);  $t_{(8060)} = 7.04$ ;  $P < 0.001$ ; Supplementary Table 1 and Fig. 2b,c). This control task therefore confirmed that human participants were able to report the expected error as well as use it to inform decision-making within our model.

### A speed–efficiency trade-off constrains sampling behaviour.

In a separate, counterbalanced session, the same participants also underwent the active version of the task, which was the main focus of our study (experiment 1b; see Methods). In this condition, they were asked to actively sample the search space before deciding where to place the blue circle in order to win credits (Fig. 1a). Both  $R_0$  and  $\eta_s$  were manipulated in a two-by-two block design ( $\eta_e$  and  $t_{\max}$  were fixed; Extended Data Fig. 2).

The game was designed such that at any given stage some candidate samples carried useful information (that is, they greatly reduced the expected error) while others did not (Extended Data Fig. 3). For example, sampling between dots of the same colour or more than two radiuses away from a purple dot did not provide any new information (that is, change in expected error = 0). As a result, the expected error could decay more or less sharply over successive observations, depending on the quality of the agent's choices of sampling locations. We quantified this dimension of behaviour (sampling efficiency) with the information extraction rate,  $\alpha$ , which was estimated separately for each trial (see Methods; Fig. 1c). This parameter quantifies the rate of exponential decay of uncertainty over successive samples (Extended Data Fig. 4). Throughout the paper, a greater value of  $\alpha$  represents a sharper expected error reduction from one sample to the next (that is, more efficient information gathering).

Unlike in many existing experimental paradigms<sup>1,5,13,18,26,27</sup>,  $\alpha$  was not imposed or fixed in our task. Instead, participants had agency over the efficiency of their own exploration strategy. At any stage of the search, they could choose to deliberate longer to acquire a sample at a more informative location, which in turn would result in

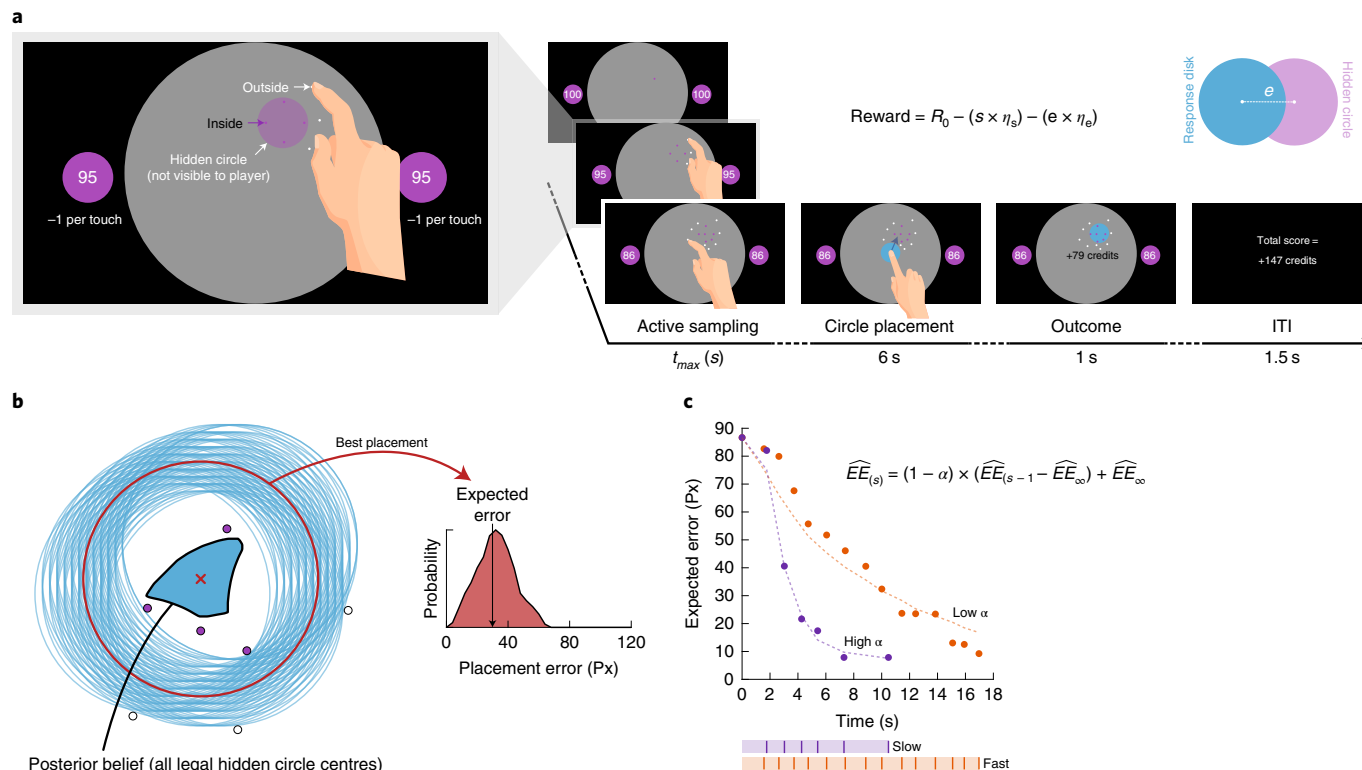


**Fig. 1 | Active information-gathering task, with large and complex sampling space.** **a**, In our experimental paradigm, people search spatially for a hidden circle, by touching screen areas, before committing to an answer. The hidden circle is 5.80% the size of the arena. They win credits as a function of the number of samples used ( $R_0 - (s \times \eta_s)$ ) and the precision of their response ( $e \times \eta_e$ ). **b**, For any visual display, the posterior belief is the set of all locations with equal, non-zero probability of being the centre of the hidden circle. The expected error is the probability-weighted average of all possible errors an agent could incur by placing the blue disk at the best possible location (the centroid of the posterior belief; red circle). White dots show samples located outside the hidden circle; purple dots show samples inside the circle. **c**, The large sampling space allows for many ways to gather information (that is, reduce the expected error). The information extraction rate,  $\alpha$ , quantifies the sampling efficiency (that is, how much expected error decays from one sample to the next). It was estimated by fitting this simple exponential relationship to individual trials (see Methods). For illustration purposes, a slow, efficient (purple) and fast, inefficient (amber) trial are plotted. Extended Data Fig. 3 illustrates the evolution of the posterior belief over the first six samples of these example trials. Extended Data Fig. 4 shows the average reduction in expected error over successive samples. Hand icon adapted from Freepik: macrovector.

a sharper reduction of uncertainty. Regardless of the experimental variable manipulated ( $R_0$  or  $\eta_s$ ), a slower acquisition rate (that is, a greater inter-sampling interval, ISI) was indeed systematically associated with more efficient sampling in experiment 1b (LMM; main effect of the natural log (ln)-transformed ISI on  $\alpha$ :  $t_{(4606)} = 10.16$ ;  $P < 0.001$ ; Supplementary Table 2 and Fig. 3a). Further analysis of the strategies underlying exploration behaviour suggested that time-dependent efficiency benefits involve both the inhibition of unhelpful automatic sampling actions and a closer approximation of the optimal search algorithm (details in Supplementary Results).

**A model of active sampling penalizing speed and efficiency.** The existence of the trade-off illustrated in Fig. 3a allowed us to ask the central question of this paper: how do humans choose the speed and efficiency at which to gather information before making a decision? Furthermore, when do they prioritize speed over efficiency (or vice versa)? And can they sometimes prioritize both?

From an optimal control<sup>28–30</sup> perspective, solving this problem requires assigning a subjective cost to both sampling speed and efficiency. Figure 4 illustrates this framework. The expected utility is calculated as the reward available (remaining credits =  $R_0 - (\eta_s \times s)$ ) minus  $(\eta_e \times EE)$  minus a cumulative cognitive effort penalty ( $\eta_c \times s$ ). We posit that the rate at which this cognitive effort penalty grows over successive samples ( $\eta_c$ ) may be a function of the sampling speed (1/ISI) and/or efficiency ( $\alpha$ ). Within this framework, a rational

decision maker chooses the course of action (a combination of sampling speed, efficiency and extent) that maximizes return (that is, the expected utility at the time of the decision). In experiment 1b, an increase in  $R_0$  should therefore not affect behaviour much because it merely influences the magnitude of the expected utility but not the course of action required to maximize it. By contrast, an increase in  $\eta_s$  should act as an incentive to sample less, slower and more efficiently, to compensate for the additional loss incurred at each step of the search.

The raw behavioural data in experiment 1b were qualitatively consistent with the predictions of this framework (Fig. 3b–d). When acquiring samples was more expensive, participants indeed explored less extensively, choosing to make fewer samples (LMM; main effect of  $\eta_s$  on the number of samples acquired:  $t_{(4604)} = -18.64$ ;  $P < 0.001$ ; Supplementary Table 3 and Fig. 3d). Remarkably, they also slowed down their exploration (LMM; main effect of  $\eta_s$  on the ln-transformed ISI:  $t_{(4604)} = 13.83$ ;  $P < 0.001$ ; Supplementary Table 4; Fig. 3b) and became more efficient, as indexed by  $\alpha$  (LMM; main effect of  $\eta_s$  on ln-transformed  $\alpha$ :  $t_{(4604)} = 2.54$ ;  $P = 0.011$ ; Supplementary Table 5; Fig. 3c). Participants also showed a very small but significant sensitivity to the starting credit: they sampled slightly faster (LMM; main effect of  $R_0$  on the ln-transformed ISI:  $t_{(4604)} = -3.94$ ;  $P < 0.001$ ; Supplementary Table 4 and Fig. 3b) and more extensively (LMM; main effect of  $R_0$  on the number of samples acquired:  $t_{(4604)} = 7.08$ ;  $P < 0.001$ ; Supplementary Table 3 and

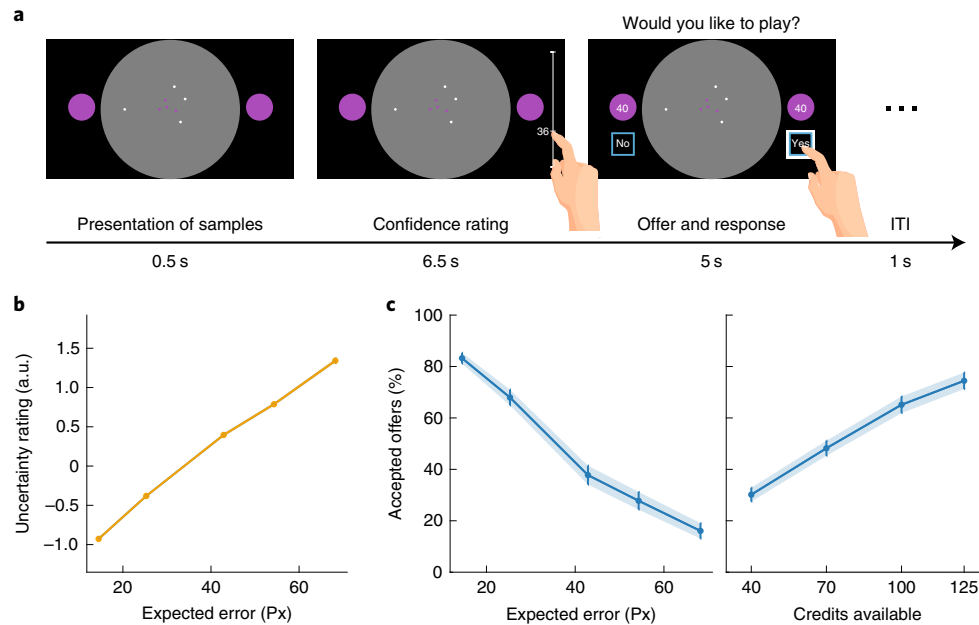


**Fig. 2 | A passive counterpart of the game shows that participants are sensitive to reward and uncertainty.** **a**, In experiment 1a, a passive version of the task was used to characterize how uncertainty (expected error) is (1) perceived (confidence rating) and (2) combined with reward into a subjective value (accept-reject decisions). ITI, inter-trial interval. **b**, Participants ( $n=48$ ) reported an uncertainty estimate that closely resembled the expected error (expected error  $\times$  uncertainty score: standardized  $\beta=0.80$ ; 95% CI = (0.76, 0.83);  $t_{(8062)}=49.89$ ;  $P<0.001$ ). **c**, They were also more likely to accept placing the blue circle when the expected error was low (main effect of expected error on decision to accept the offer: standardized  $\beta=-2.53$ ; 95% CI = (-2.80, -2.27);  $t_{(8060)}=-8.57$ ;  $P<0.001$ ) and the number of credits available was high (main effect of reward on decision to accept the offer: standardized  $\beta=1.87$ ; 95% CI = (1.49, 2.26);  $t_{(8060)}=7.04$ ;  $P<0.001$ ). In **b** and **c**, the dots show group means and the error bars show s.e.m. Full statistical details are reported in Supplementary Table 1. Hand icon adapted from Freepik: macrovector.

Fig. 3d) when more reward was available. This sensitivity effect should not exist if economical variables are represented veridically (rational decision maker) and may instead reflect the use of a nonlinear utility function. For completeness, the effects of all of the experimental variables on the placement error and score are reported in Supplementary Tables 7 and 8.

To formally assess whether positing a cognitive effort cost in terms of sampling speed and efficiency was indeed required to explain human behaviour quantitatively in our task, we fitted variants of our proposed modelling framework to individual datasets. Model fitting required the introduction of free parameters to the framework, estimated at the individual level. All of the models included two free weights,  $w_e$  and  $w_s$ , which quantified the influence of information-related benefits and the sampling cost to the expected utility, respectively (Fig. 4b; see Methods). The reference model (model 1) included no cognitive effort cost at all and was in effect similar to standard views that do not account for this factor. Because it is known that humans often exhibit nonlinear utility functions when deciding under uncertainty<sup>11</sup>, as suggested here by the small sensitivity to the starting credit (Fig. 3b–d), we first evaluated a model with a power term on the sampling cost (model 2). In this model, the sampling speed and efficiency were not penalized, but the contribution of sampling costs to the expected utility could increase or decrease nonlinearly as a function of the number of samples acquired (details in Methods). This was used as a second reference model to check whether a nonlinear utility function could account for the data in the absence of cognitive effort cost.

The subsequent models (models 3–14) evaluated the four classes of cognitive effort cost depicted in Fig. 4c: linear, quadratic, exponential and sigmoid. Thus, they differed with respect to how sampling speed ( $1/ISI$ ) and efficiency ( $\alpha$ ) were penalized. Note that exponential and logistic cost functions required an extra free parameter relative to linear and quadratic ones (see Methods and

Extended Data Fig. 5). To avoid over-fitting by overly complex models, a veridical specification of economic variables was used when a cognitive effort cost was included (that is, there was no power term on sampling cost in models 3–14). For each class of cost function, three versions of the model were built, based on whether speed, efficiency or both were penalized. The free weights  $w_{\text{speed}}$  and  $w_\alpha$  quantified how severely the sampling speed and efficiency, respectively, were penalized within the cognitive effort cost function. The latter also included a free intercept,  $w_0$ . Free parameters were estimated separately for each individual dataset using a maximum (multivariate) likelihood procedure that was implemented in MATLAB with Bayesian adaptive direct search<sup>31</sup>. Model comparison was carried out with the Bayesian information criterion (BIC), which was chosen for its stringent penalization of model complexity. A smaller BIC indicates a better trade-off between model fit and complexity.

In the absence of a cognitive effort cost, positing a nonlinear utility function provided a better account of the data than a purely rational specification (model 2 versus model 1:  $\Delta\text{BIC}=-1,036$ ; Fig. 5a). However, this was a rather small explanatory power benefit compared with those observed with models including a cognitive effort cost (models 3–14). Overall, the winning model (model 8) penalized for both speed and efficiency using a quadratic cost function (model 8 versus 1:  $\Delta\text{BIC}=-22,779$ ; Fig. 5a). The winning cognitive effort cost function was:

$$\eta_c(\text{ISI}, \alpha) = w_0 + w_{\text{speed}} \times \frac{1}{\text{ISI}^2} + w_\alpha \times \alpha^2 \quad (\text{quadratic}) \quad (1)$$

Thus, as expected, positing the existence of a cognitive effort cost, due to both a cost of speed and a cost of efficiency, improved our ability to explain participants' choices of sampling speed, efficiency and extent in experiment 1b (see Supplementary Fig. 2 for other models that did not outperform model 8).

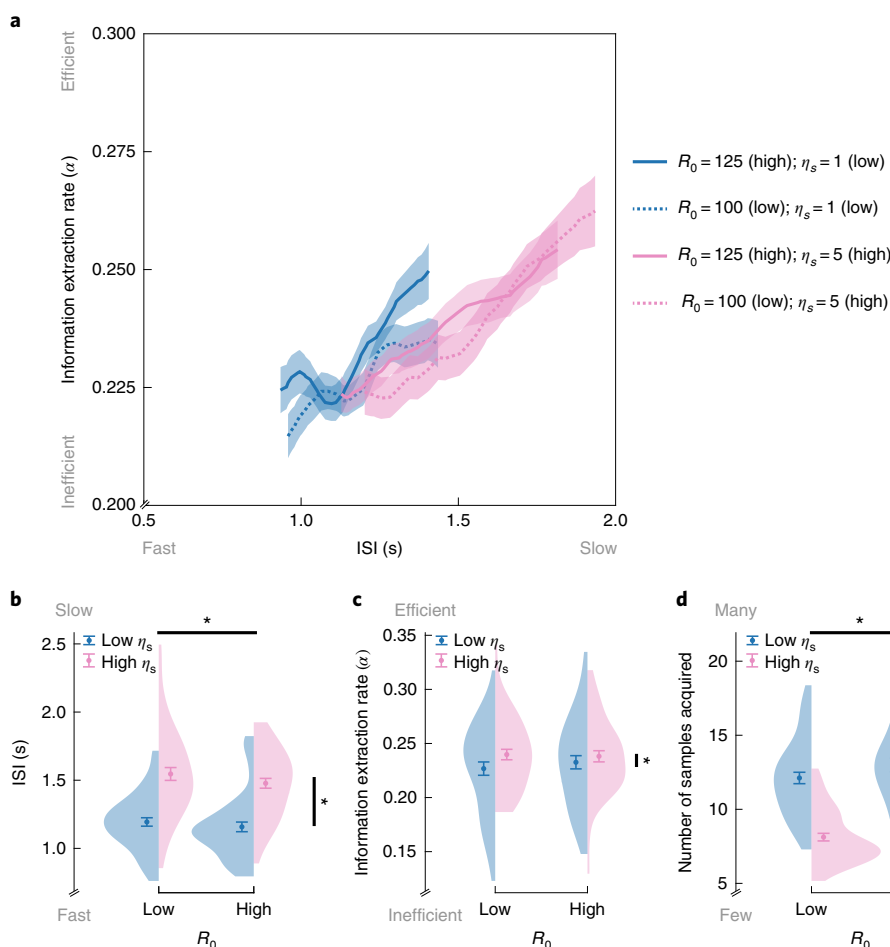


**Fig. 3 | Economic and time constraints influence the extent, speed and efficiency of active information sampling.** **a**, Across all four experimental conditions of experiment 1b ( $n = 48$  participants), a slower sampling rate (longer ISI) led to sharper reductions of uncertainty from one sample to the next (larger  $\alpha$ ; main effect of ln-transformed ISI on  $\alpha$ :  $t_{(4606)} = 10.16$ ;  $P < 0.001$ ). The ISI and  $\alpha$  were calculated separately for each trial. Conditional plots were generated by sliding, for each subject and condition separately, 25% quantile bins of ISI and computing the mean  $\alpha$  for each bin. The shading shows the group s.e.m. **b–d**, Participants sampled slower (**b**) and more efficiently (**c**) but less extensively (**d**) when acquiring data was more expensive (high  $\eta_s$  (pink) versus low  $\eta_s$  (blue)). In contrast, a larger starting credit led to a small increase in the sampling speed and the amount of data acquired but had no significant effect on efficiency (high versus low  $R_0$ ). Points and error bars show group means  $\pm$  s.e.m. Asterisks show significant effects (vertical bars = main effect of  $\eta_s$ ; horizontal bars = main effect of  $R_0$ ;  $P < 0.05$ ). Full statistical details are reported in Supplementary Tables 2–6.

A potential limitation of the winning model is that, unlike in simple motor tasks<sup>32</sup>, the intrinsic relationship between speed and efficiency is poorly understood here. As a result, the addition of the degrees of freedom we proposed might merely reflect the need for the model to incorporate a specification of this relationship, rather than a true cognitive effort cost. The last two sections provide evidence in favour of the existence of a true cognitive effort cost that influences active information sampling.

**Efficiency penalties reflect a cognitively effortful process.** To seek independent confirmation that the cost introduced in our framework indeed captures an effortful process, participants were asked to rate, on a visual analogue scale, how tired they felt throughout the experimental session in experiment 1b (see Methods). On average, fatigue built up linearly over successive task blocks (LMM; main effect of the block on fatigue ratings:  $t_{(1150)} = 4.16$ ;  $P < 0.001$ ; Supplementary Table 9 and Fig. 6a). Importantly, the amount by which it increased showed a significant association with the contribution of efficiency to individuals' cognitive effort cost ( $w_\alpha$ , as extracted through model fitting; see Methods). Those participants in whom increasing the efficiency was subjectively more costly

(high  $w_\alpha$ ) also suffered a greater increase in subjective fatigue as a result of performing the task (standardized  $\beta = 0.49$ ; 95% CI = (0.17, 0.80);  $t_{(43)} = 3.13$ ;  $P = 0.0032$ ; robust multiple linear regression controlling for  $w_0$ ,  $w_{\text{speed}}$  and experiment duration; Supplementary Table 10 and Fig. 6b). By contrast, those for whom increasing the sampling efficiency was less penalized became less tired over the course of the experiment. Performing the analysis on z-scored ratings did not change the conclusion (Supplementary Tables 9 and 10). Thus, the efficiency cost introduced in our modelling framework captures an effortful process that was meaningfully related to how subjective fatigue developed throughout the task.

**Breaking the speed–efficiency trade-off under time pressure.** A second way to adjudicate whether the speed–efficiency trade-off we uncovered involves a cognitive effort cost is to ask whether it is breakable under certain experimental conditions. If the trade-off solely reflects the fact that sampling efficiency is naturally a function of speed, participants should be constrained to manipulating these two dimensions in an anti-correlated fashion. In other words, sampling faster comes at the cost of efficiency, and vice versa. If, alternatively, the trade-off emerges from a cognitive effort

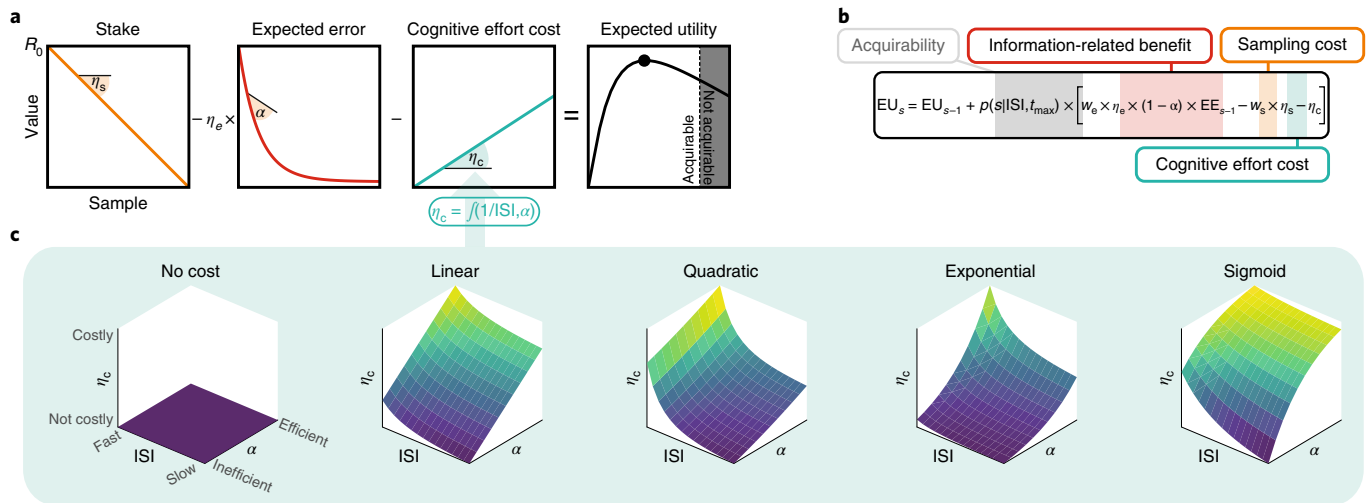


**Fig. 4 | Choosing how quickly, efficiently and extensively to sample.** **a**, Standard accounts of active information sampling posit that individuals behave so as to maximize the expected value of the decision, which is calculated here as  $R_0 - (\eta_s \times s) - (\eta_e \times EE)$  (see also Supplementary Fig. 3). This formalism is useful to decide how many samples to acquire but cannot predict how quickly or efficiently to sample. To do so, we propose to introduce a cognitive effort cost,  $\eta_c$ , which agents have to pay for each sample acquired and which may be a function of both the sampling speed ( $1/ISI$ ) and/or efficiency ( $\alpha$ ). **b**, The expected utility is then defined as the previous expected utility plus the expected information-related benefit that would result from sampling minus the  $\eta_s$  and  $\eta_c$  expended in finding the sample. The acquirability equals 1 for samples obtainable during the time allocated to the search, and 0 otherwise. **c**, Various candidate cognitive effort cost functions were evaluated in this paper (linear, quadratic, exponential and logistic). When  $\eta_c = 0$  (models 1 and 2), our framework reduces to previous accounts. Other models (models 3–14) differ in the way sampling speed ( $1/ISI$ ) and efficiency ( $\alpha$ ) are penalized.

cost, under sufficient experimental pressure, participants should be able to increase speed without sacrificing efficiency, or vice versa, or even increase both at the same time. Note that these two hypotheses are not mutually exclusive and the key prediction is that of a breakable trade-off if a cognitive effort cost contributes to information-sampling behaviour.

To test whether the speed–efficiency trade-off could be broken in some conditions, the four experimental variables ( $R_0$ ,  $\eta_s$ ,  $\eta_e$  and  $t_{max}$ ) were manipulated in isolation in four separate experiments (experiments 2–5;  $n = 79$  participants divided into four groups; mean age = 25.13 years; s.d. = 4.05 years; see Methods and Extended Data Figs. 1 and 2). Full statistical analysis of sampling behaviour for these experiments is provided in the Supplementary Results (Extended Data Fig. 6). None of the economic variables ( $R_0$ ,  $\eta_s$  and  $\eta_e$ ; experiments 2–4) led to violations of the speed–efficiency trade-off (Fig. 7). That is, even when they adjusted speed and efficiency in response to changes in  $\eta_s$  (Figs. 3a and 7), individuals remained confined within a fixed anti-correlation between the two. This was evidenced by the disappearing of the effect of  $\eta_s$  on  $\alpha$  when controlling for sampling speed in experiment 3 (LMM; main effect of  $\eta_s$  on ln-transformed  $\alpha$ :  $t_{(1918)} = 3.97$ ;  $P < 0.001$ ; Supplementary Table 5; main effect of  $\eta_s$  on ln-transformed  $\alpha$  while controlling for ln-transformed ISI:  $t_{(1917)} = -0.60$ ;  $P = 0.55$ ; Supplementary Table 6; also observed in experiment 1b).

By contrast, time pressure (small  $t_{max}$ ) acted as a drive for participants to break the speed–efficiency trade-off. In experiment 5 ( $n = 19$  participants), the time available for people to sample before making their final decision ( $t_{max}$ ) was either 18 s (as in the previous experiments) or 14, 10 or 6 s (Extended Data Fig. 2). Compared with experiments in which economic variables were individually manipulated ( $R_0$ ,  $\eta_s$  and  $\eta_e$  in experiments 2–4;  $n = 60$  participants), players under overall heightened time pressure sampled on average not only faster (LMM; contrast experiment 5 versus experiments 2–4 for ln-transformed ISI:  $F_{(1,7580)} = 47.65$ ;  $P < 0.001$ ) but also more efficiently (LMM; contrast experiment 5 versus experiments 2–4 for ln-transformed  $\alpha$ :  $F_{(1,7580)} = 5.26$ ;  $P = 0.022$ ; Fig. 7a). In other words, they broke the speed–efficiency trade-off observed in previous experiments.

Because this result relies on a between-group comparison, we checked that it could not be accounted for by inter-individual differences in IQ (Raven’s progressive matrices<sup>33</sup>) or self-reported motivation indices of apathy (apathy motivation index<sup>34</sup>) and impulsivity (Barratt impulsiveness scale-11; ref. <sup>35</sup>). Including these external measures within the previous analysis made no difference to the result (LMM; contrast experiment 5 versus experiments 2–4 for ln-transformed ISI while controlling for questionnaires:  $F_{(1,7577)} = 48.30$ ;  $P < 0.001$ ; contrast experiment 5 versus experiments 2–4 for ln-transformed  $\alpha$ :  $F_{(1,7577)} = 4.82$ ;  $P = 0.028$ ). Furthermore (and crucially), even within experiment 5, there was evidence of a breaking of the speed–efficiency trade-off at the within-individual level. A shorter  $t_{max}$  led to faster sampling (LMM; main effect of  $t_{max}$  on ln-transformed ISI:  $t_{(1822)} = 11.71$ ;  $P < 0.001$ ; Supplementary Table 4) with no significant loss in terms of efficiency (LMM; main effect of  $t_{max}$  on ln-transformed  $\alpha$ :  $t_{(1822)} = -0.02$ ;  $P = 0.98$ ; Supplementary Table 5). This time, when controlling for sampling speed in the analysis,  $\alpha$  showed a significant increase with shorter  $t_{max}$  (LMM; main effect of  $t_{max}$  on ln-transformed  $\alpha$  while controlling for ln-transformed ISI:  $t_{(1821)} = -3.86$ ;  $P < 0.001$ ; Supplementary Table 6).

Taken together, the results demonstrate that participants could break the speed–efficiency trade-off, sampling both faster and more efficiently. This qualitative feature can be seen as a direct manifestation of the existence of cognitive effort cost (Fig. 4). Formal model comparison for experiments 2–5 confirmed this conclusion, replicating the results of experiment 1b. Once again, human performance was best explained when positing the existence of a quadratic cognitive effort cost penalizing both speed and efficiency (model 8 versus model 1:  $\Delta BIC = -37,800$ ; Fig. 5b and Extended Data Fig. 7). Taken together, our results suggest that the way humans seek knowledge to guide their decisions is shaped not only by the economic costs and benefits of information, but also crucially by the cognitive effort expenditure involved in seeking this information.

## Discussion

Modern theories of active sampling assume that the brain optimizes the amount of information needed before decision-making on the

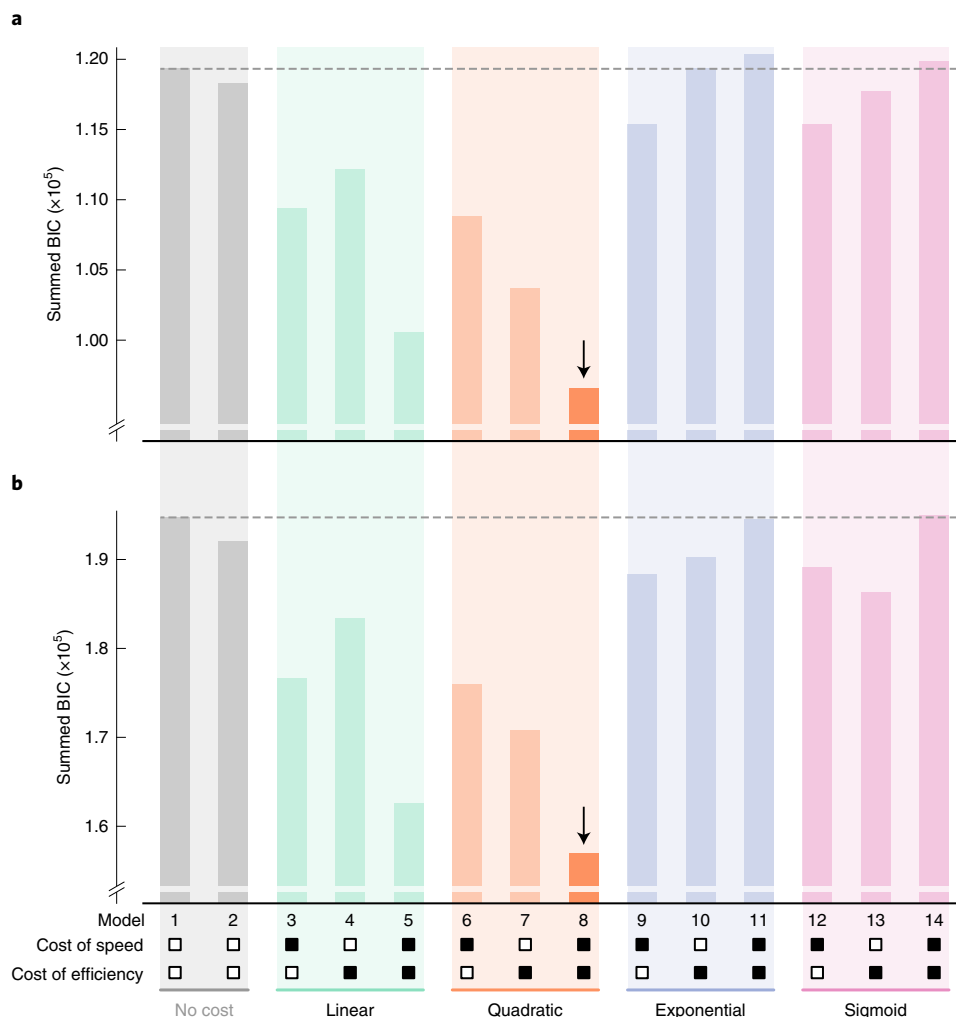


**Fig. 5 | A model comparison robustly shows, across five experiments, that a model with a quadratic cognitive effort cost best explains active information-sampling behaviour.** Models 1 and 2 included no cognitive effort cost (model 1 = rational specification; model 2 = nonlinear utility function; in grey) and were used as references. The other 12 models included a cognitive effort cost specified in terms of either speed (models 3, 6, 9 and 12), efficiency (models 4, 7, 10 and 13) or both (models 5, 8, 11 and 14). For each cost (speed and efficiency), the squares below the x-axis represent whether or not it was included in the model (black, included; white, not included). Models also differed with respect to the shape of the cognitive effort cost function used (green, linear; orange, quadratic; blue, exponential; pink, sigmoid). The dashed line represents the BIC of the reference model (smaller BIC is better). **a**, In experiment 1b ( $n = 48$  participants), individuals' choices of sampling speed, efficiency and extent were best explained by a model penalizing both speed and efficiency with a quadratic cost function (model 8; lowest BIC). **b**, Model comparisons from experiments 2–5 (BIC summed across all four experiments;  $n = 79$  participants) replicated the winning model from experiment 1b (model 8). This was also the case when considering each experiment separately (Extended Data Fig. 7).

basis of the costs and benefits of resolving uncertainty. Accordingly, informative samples are worth acquiring only when the subjective benefits they provide outweigh the cost of obtaining them. This simple axiom has proven extremely powerful in explaining how much information people seek before decision-making<sup>4,5,6,12–17</sup>, and provides a theoretical bridge to other types of motivated behaviours such as foraging<sup>4,36,37</sup>. However, a natural key question is: what do people treat as costs and benefits during active information sampling?

Here, we focused on one cost whose contribution has been elusive so far—the cognitive effort cost<sup>19,20</sup>. We hypothesized that if the brain discounts the cognitive effort expended from information benefits, active sampling behaviour should be more flexible than is currently assumed. More specifically, if finding more informative samples comes at an extra cognitive cost, people should search fast and efficiently only when pressured by task constraints. Using a complex active sampling experimental paradigm, we showed that

humans indeed flexibly adjust the amount of cognitive resources they allocate to active sampling, in response to economic and time pressures. They sample more efficiently but slower when the economic losses incurred increase (experiment 1b and 3), and are able to break this trade-off under time pressure, sampling both faster and more efficiently (experiment 5; Fig. 7).

To account for this flexibility, we posited the existence of a cognitive control mechanism<sup>22,38</sup> that determines how quickly and efficiently to sample information. Importantly, in this cost-benefit evaluation, both speed and efficiency are treated as costly. Incorporating this notion into a standard information-sampling model explained human behaviour better than simpler models. Further confirmation of the psychological validity of our framework was provided by the significant relationship between subjective fatigue reports and the model-derived cost of efficiency (Fig. 6). These findings have some resonance with existing behavioural theories that invoke cognitive effort to explain why consumers

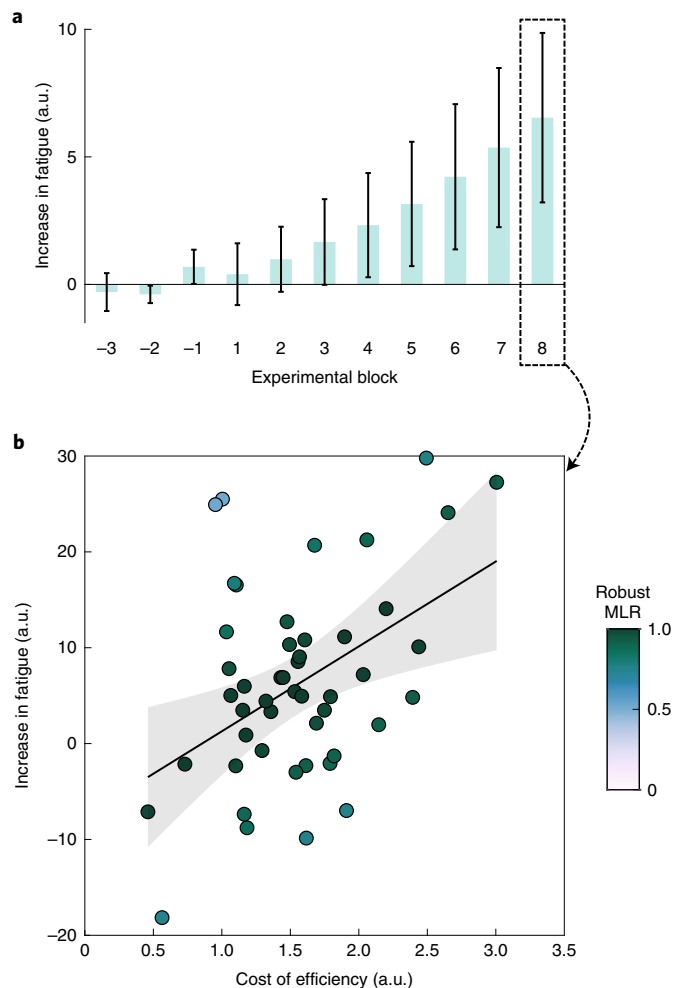


**Fig. 6 | The cost of efficiency is associated with fatigue development.**

**a**, In experiment 1b, participants ( $n = 48$ ) rated how tired they felt throughout the experimental session. The average rating during the exposure task (blocks  $-3$  to  $-1$ ) was used as the baseline fatigue, which was subtracted from subsequent ratings for normalization purposes. On average, fatigue increased linearly over successive blocks (main effect of block on fatigue ratings:  $t_{(1150)} = 4.16$ ;  $P < 0.001$ ). Bars and error bars show group means with 95% confidence interval. **b**, The cost of efficiency ( $w_e$ ) was associated with the increase in fatigue observed as a result of the experimental session (standardized  $\beta = 0.49$ ; 95% CI =  $(0.17, 0.80)$ ;  $t_{(43)} = 3.13$ ;  $P = 0.0032$ ; robust multiple linear regression controlling for  $w_0$ ,  $w_{\text{speed}}$  and experiment duration). The scatter plot shows the mean normalized fatigue rating in the last experimental block (y-axis) as a function of the cost of efficiency ( $w_e$ ), controlling for task duration,  $w_0$  and  $w_{\text{speed}}$  (task duration,  $w_e$  and  $w_{\text{speed}}$  were ln-transformed for normalization purposes). The colouring shows the contribution of individual data points to the robust multiple linear regression (MLR) (multivariate outliers are downweighted). The solid line and error shading show the linear regression line with 95% confidence interval. Full statistical details are reported in Supplementary Tables 9 and 10.

do not compare products that differ along multiple dimensions<sup>39</sup>, or why they do not read contracts<sup>40</sup>. Within a very distinct situation (one in which people have to actively sample their environment in order to reduce uncertainty about a spatial dimension) we have demonstrated that similar principles may apply. Crucially, however, the model provided here is quantitative and accounts for changes in behaviour (that is, it generates quantifiable predictions of sampling behaviour that are testable experimentally).

Consistent with current theories of control allocation in other domains<sup>30,41</sup>, our results converged on the view that the brain actually penalizes fast and efficient information sampling, thereby promoting what is effectively sub-optimal exploration in the absence of strong environmental pressure. It was evident that under greater time pressure, individuals could sample faster and more efficiently, but chose not to do so when there was a longer deadline (Fig. 7). There are at least three possible reasons why such a mechanism might exist: metabolic cost, shared computing resources and reliability testing. First and foremost, fast and efficient sampling might increase metabolic consumption because of additional neural resources requirements (for example, a higher neural firing rate<sup>42</sup>, optimization of brain network organization<sup>43,44</sup> or more efficient information processing<sup>25,45</sup>). An indirect proxy for such a possible increase in (metabolically costly) processing demands was provided by the analysis of choices of sampling location, which supported the flexible switching between search algorithms of various computational complexity<sup>46,47</sup> (see Supplementary Results).

The second explanation is that, because other cognitive processes also depend on the same shared limited neural resources, prioritization of one process might negatively impact on the others, resulting in an opportunity cost in terms of unprocessed task-unrelated stimuli<sup>22</sup>. In this context, sub-optimal sampling performance might leave room (capacity) for parallel processing of other potentially useful information. Finally, although it impinges on search efficiency, there might be indirect benefits to acquiring apparently uninformative, confirmatory samples<sup>48</sup>. Indeed, they provide timely checks of the reliability of the information source that can only be performed where the agent has perfect knowledge over what the outcome should be (that is, null entropy). Challenging what is already known might confer an ecological advantage in non-deterministic environments where the trustworthiness of past and future observations may drift over time.

The computational framework used throughout this paper assumes that individuals choose how to explore (that is, how quickly, efficiently and extensively to sample) on the basis of internal simulations of what the future might hold for all alternative courses of action—or at least a simplified, representative sub-sample of them<sup>49</sup>. This principle is well-established within the sensorimotor control<sup>50</sup> and goal-directed<sup>51</sup> literature. Deciding within this strategy space therefore requires metacognitive abilities<sup>52,53</sup> that may only be acquirable through experience (for example, an expectation of the actual uncertainty reduction for a given internally selected efficiency,  $\alpha$ ; an expectation of the actual error for a response under a certain uncertainty level). It is possible that this meta-knowledge may, to a certain extent, be learnt online as participants try out various strategies (see Supplementary Information for a visualization of behaviour as a function of task exposure). This idea is compatible with a recent account of cognitive control in which a reinforcement meta-learner learns how to select behavioural states (for example, physical/cognitive effort) through error-based updating coupled with value-based action selection<sup>54</sup>. Our experimental paradigm could therefore be used in the future to investigate the computational architecture underlying de novo learning of a cognitive effort cost function.

Previous information sampling tasks (for example, the card sampling task<sup>18</sup>, tile flipping task<sup>1</sup>, beads/urn task<sup>26</sup> and dart/fishing task<sup>5</sup>) could not isolate cognitive effort cost from mere economic sampling cost because participants had little to no control over the efficiency of their search (here parameterized as  $\alpha$ ). If all candidate samples are expected to reduce uncertainty by the same amount, regardless of the time or cognitive effort spent choosing them, active sampling becomes solely about whether or not to sample (that is, when to stop). Cognitive effort needs to confer an instrumental advantage for it to be traded against other resources<sup>41</sup>. However, it is worth emphasizing that in the simpler instance where  $\alpha$  is constant, our active sampling model actually reduces to



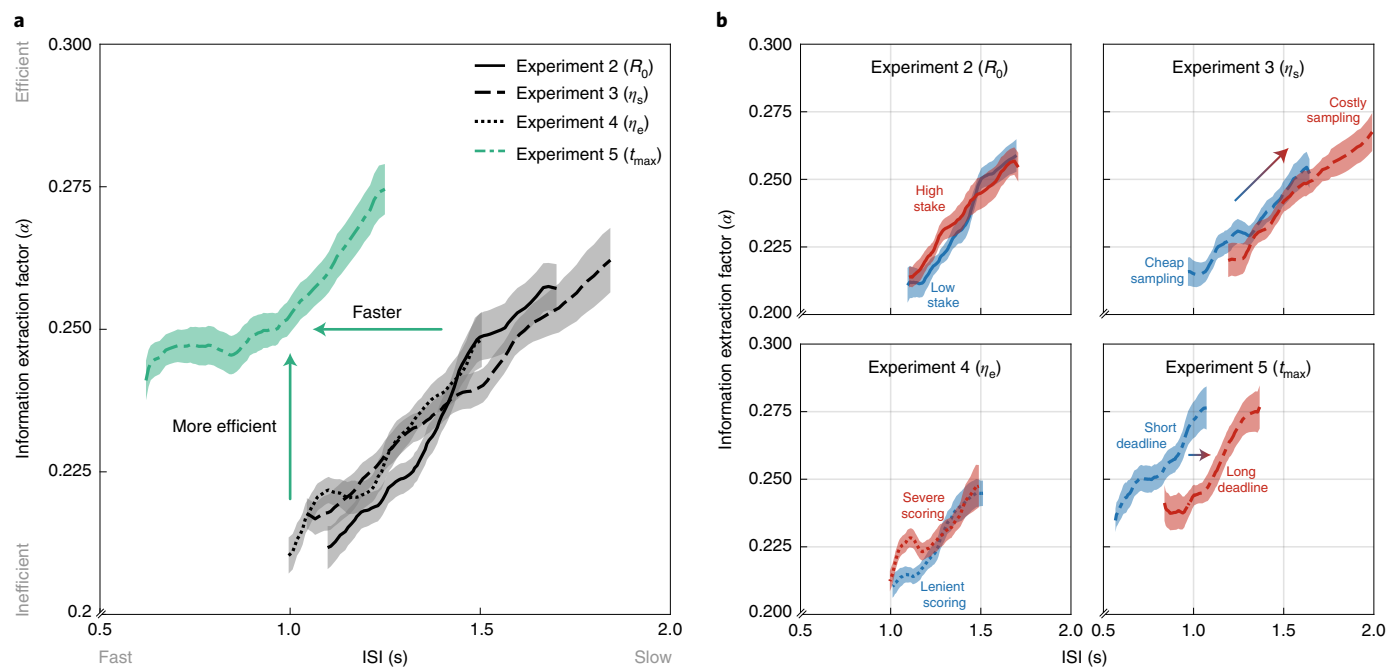


**Fig. 7 | A breakable speed-efficiency trade-off governs active information sampling.** **a**, Overall, in experiments 2–5 ( $n = 79$  participants), longer ISIs led to larger information gains at each step, as in experiment 1b. However, participants of experiment 5 ( $n = 19$ ; green dot-dashed line) were able to sample both faster (contrast experiment 5 versus experiments 2–4 for In-transformed ISI:  $F_{(1,7580)} = 47.65$ ;  $P < 0.001$ ) and more efficiently (contrast experiment 5 versus experiments 2–4 for In-transformed  $\alpha$ :  $F_{(1,7580)} = 5.26$ ;  $P = 0.022$ ; Extended Data Fig. 6). In the framework we propose (Fig. 4), maintaining the same level of efficiency while sampling faster, or extracting more information for a given ISI, are considered to be cognitively effortful (for example, these actions consume more energetic resource). These costs are captured by the model parameters  $w_{speed}$  and  $w_{\alpha}$ . **b**, To visualize the effect of economic (experiments 2–4) and time pressures (experiment 5) on the speed-efficiency trade-off, the same plot was generated for each experimental condition (highest and lowest two levels grouped together). Individuals lost in speed what they gained in efficiency when sampling costs increased (experiment 3), but were able to break this trade-off under time pressure (experiment 5). In **a** and **b**, the conditional plots were generated by sliding, for each subject and condition separately, 25% quantile bins of ISI and computing the mean  $\alpha$  for each bin. In **a** and **b**, shading represents the s.e.m. Full statistical details are reported in Supplementary Tables 4–6.

previous accounts<sup>5,17</sup> (Fig. 4). In contrast, if agents have control over the informativeness of individual samples, as in the active sampling task introduced here and most real life scenarios, optimal allocation of computational resources becomes a central problem, which our model offers a solution to.

Our study has three main limitations. First, the task relies heavily on motor performance, both to sample the search space and to produce a response at the end of every trial (Fig. 1a). Inter-individual differences in motor abilities may affect performance in ways that are not (or wrongly) captured by the model (Fig. 4). Although this source of variance is likely to be negligible in the population of young healthy adults tested here, it may become a more significant confound in certain age groups or clinical populations. Second, the definition of uncertainty used throughout this work (expected error) relies on the assumption that people were able to use all of the information that was available in the visual display. However, it can be argued that the level of uncertainty depends not only on the information presented (that is, the visual display) but also the agent's ability to use this information (that is, which solution they select within the solution space). Thus, for the same visual display, an individual who is well able to identify the best solution within the solution space should rightly expect a lower error than an individual who typically picks worse solutions. For simplification purposes, and because the expected error provided a good estimate of actual placement errors (Supplementary Fig. 1), this layer of complexity was omitted in the present work. Lastly, the model developed here assumes a constant sampling speed and efficiency within a given trial and therefore cannot account for within-trial effects

(for example, speeding up or slowing down as individuals get closer to the decision deadline). Considering within-trial effects may allow future studies to better characterize dynamic decision processes unfolding during the exploration. More specifically, it may enable the segregation of two distinct decisions: (1) whether or not to sample; and (2) where to sample.

In conclusion, the results presented here identify cognitive effort as a central cost that the brain trades off against reward during active information sampling before decision-making under uncertainty. The active sampling experimental model introduced here, together with our modelling approach, offers a compact way to quantify the contribution of this cost.

## Methods

**Participants.** All participants provided written informed consent and the study was approved by the University of Oxford ethics committee. Sample size was determined a priori based on counterbalancing constraints and previous studies with similar objectives<sup>5,35,36</sup>. Recruitment took place via the Oxford Psychology Research participant recruitment scheme website (<https://opr.sona-systems.com/>) and via online study advertisement. Participating in an experiment was a criterion of exclusion for the other experiments, such that there was no overlap in participants between experiments 1–5. Volunteers were predominantly university students and young professionals. None of them reported taking psycho-active drugs or having a personal history of a neurological or psychiatric condition.

Experiment 1 included 48 participants (24 females); experiments 2–4 included 20 participants each (ten females per experiment); and experiment 5 included 19 participants (ten females). Thus, in total, 127 different participants were tested in this work. Demographics and participant characteristics are reported in Extended Data Fig. 1. In experiment 1, prospective volunteers (148 individuals volunteered) were selected based on their motivation level, gender and age, to ensure a large

spread of motivational levels. The online screening questionnaire included the apathy motivation index (AMI), a validated self-report index of apathy and motivation<sup>34</sup>, and demographics information (gender, age, years of education, handedness, medication and personal history of neurological or psychiatric conditions). No participant dropped out after inclusion and all tested participants were included in the analysis.

**Apparatus.** All of the tasks were presented on a 17-inch touchscreen PC using MATLAB version 2018a (MathWorks; <https://uk.mathworks.com>) and Psychtoolbox<sup>37,38</sup> version 3. Participants sat in a quiet room within reaching distance of the screen (~50 cm). An experimenter was present in the room at all times during behavioural testing.

**Active information-sampling task (Circle Quest).** The goal of the Circle Quest task was to win as many credits as possible. Participants were instructed that the visual display contained a purple circle that was hidden behind a circular grey mask (search space). The size of the hidden circle (radius = 130 pixels; area = 5.80% of the search space) was displayed on both sides for reference. The number of credits that could be won by perfectly localizing the hidden circle was displayed on the side at all times and decreased every time participants touched the screen during the sampling phase. This quantity represented an endowment from which sampling and error costs were subtracted. When manipulated,  $\eta_c$  was visually depicted on the side as a progress bar with the words 'Scoring severity' at the top (experiment 4). This progress bar could contain one, two, three or four squares, corresponding to an error cost of 0.5, 1.5, 1.9 or 2.6 credits per pixel, respectively. This could change from one trial to the next but remained constant within a given trial. Finally, when manipulated, a timer representing the remaining time allocated to the search was displayed on both sides of the screen (experiment 5). This took the shape of a timer that filled up clockwise.

Information about the location of the hidden circle could be gathered by tapping the screen. If participants touched inside the hidden circle, a purple dot (radius = 4 pixels) appeared. If they touched outside the hidden circle, a white dot appeared. Trials comprised two phases. During the active sampling phase, participants could collect as many samples as they wanted, at any location inside the search space. They were instructed that they could stop at any moment but had to wait until the end of the allocated time before making their final response. A single purple dot was displayed on the screen at the beginning of this phase, to act as an initial hint and shorten the length of the search. The location of this first purple dot was drawn randomly from inside the hidden circle and was always at least 260 pixels away (the diameter of the hidden circle) from the edge of the search space, to ensure it always carried the same amount of information (expected error at the start of the search = 86.67 pixels). The number of credits available decreased every time participants acquired a sample. At the end of the sampling phase, a blue disk of the same size as the hidden circle (radius = 130 pixels) appeared in the middle of the screen. Participants then had 6 s to drag it on top of where they thought the hidden circle was. Finally, the score was presented. This was calculated using the formula reward =  $R_0 - (s \times \eta_i) - (e \times \eta_c)$ . Participants won all of the remaining credits ( $R_0 - (s \times \eta_i)$ ) minus a penalty reflecting how far they placed the blue disk from the actual hidden circle ( $e \times \eta_c$ ). In other words, there were two ways of losing credits in this task: (1) by sampling information; and (2) by mis-localizing the hidden circle. The duration of each trial was experimentally set such that participants could not complete more trials by sampling less/faster or placing the blue circle quickly.

**Passive decision task.** To characterize the extent to which participants were sensitive to the number of credits and expected error on offer, we designed a version of the task in which these two variables were experimentally manipulated on a trial-by-trial basis (Fig. 2a). The design of this task was inspired by other decision-making tasks developed in the laboratory<sup>55,59–61</sup>. This task was counterbalanced with the active sampling version in experiment 1.

First, participants saw dot samples on the screen. All trials contained four positive (purple) and four negative (white) samples. The uncertainty (expected error) was manipulated by varying the spatial configuration of these samples. For example, the expected error was greater when the positive samples were clustered together as opposed to spread out. The same set of stimuli were used for all individuals but the order of presentation was randomized. The expected error ranged from 10–70 pixels. Participants were asked to first report on a scale from 0–100 how confident they felt about their ability to localize the hidden circle, given the samples displayed on the screen. After the confidence rating, the number of credits available appeared (either 40, 70, 100 or 125). Participants were then asked to accept or reject the offer to place the blue circle. Note that participants simply expressed preferences in this version of the task, such that there was no correct or incorrect response. They received no feedback during their series of choices. To incentivize the context, they were instructed that a sub-sample of their accepted trials would be selected at the end of the session for them to position the blue circles and win credits accordingly.

In total, all participants underwent the same set of 168 trials (42 trials per reward level), divided into six experimental blocks (28 trials per block). The order of presentation was randomized.

**External measures.** Interleaved with the tasks, participants completed established self-report questionnaire measures of apathy (AMI<sup>34</sup>), impulsivity (Barratt impulsiveness scale-11; ref. <sup>35</sup>), depression (Beck Depression Inventory-II<sup>62</sup>) and uncertainty preference (Intolerance of Uncertainty Scale<sup>63</sup>). They also performed a time-limited (10 min) test of non-verbal fluid intelligence (Raven's progressive matrices test<sup>33</sup>).

**Fatigue ratings.** In experiment 1b, participants were asked to rate, between 0 and 100, their level of subjective fatigue at various points throughout the experimental session. When doing so, a vertical visual analogue scale appeared in the middle of the screen with the words 'Not at all' and 'Extremely' at its lowest and highest extremes, respectively, and the question 'How tired do you feel?' was displayed at the top.

Individuals were instructed to touch the screen to place a cursor at the level that best reflected their current fatigue state. The corresponding rating (a number between 0 and 100) was displayed on the side of the cursor to facilitate the response. For any given rating, the starting position of the cursor was set to the value of the preceding rating. Participants pressed the space bar to validate their response and resume the task.

Individuals were asked to rate their fatigue at the beginning, middle and end of each experimental block (that is, nine times during the exposure task then 24 times during the active sampling task). Both raw and z-scored ratings were analysed.

**Experimental design.** The average duration of each experiment is provided in Extended Data Fig. 1. Experiment 1 included two separate sessions (a passive decision task (experiment 1a) and an active information-sampling task (experiment 1b)), taking place at the same time on consecutive days. The order of the two sessions was fully counterbalanced among gender category. Then, participants underwent three blocks of 28 exposure trials (84 trials in total), requiring them to place the blue disk for different combinations of reward and uncertainty (average duration = 10.0 min; s.d. = 1.7 min; performance reported in Supplementary Fig. 1). The aim of this short task was to expose participants to the scoring function so that they could perform the passive choice experiment even on the first session. After the exposure task, participants underwent either eight blocks of 12 active sampling trials (96 total; active information-sampling task) or six blocks of 28 choice trials (168 total; passive decision task). Both the starting credit ( $R_0 = 100$  or 125 credits) and sampling cost ( $\eta_s = 1$  or 5 credits per sample) were experimentally manipulated in a two-by-two design in the active information-sampling task in experiment 1b (24 repetitions of each of the four combinations; Extended Data Fig. 2). In addition, a visual analogue scale appeared on the screen every 14 trials during the exposure task and every six trials during the active information-sampling task, for participants to rate how fatigued they felt. The average value during the exposure was used as the baseline measure of fatigue.

In experiments 2–5, all four experimental variables ( $R_0$ ,  $\eta_s$ ,  $\eta_c$  and  $t_{\max}$ ) were manipulated in separate experimental groups. They each included four blocks of 24 trials (96 trials in total). Every block featured six repetitions of each of the four levels of the experimental variable manipulated (experiment 2:  $R_0 = (50, 75, 100, 125)$  credits;  $\eta_s = 3$  credits per sample;  $\eta_c = 1.2$  credits per pixel;  $t_{\max} = 18$  s; experiment 3:  $R_0 = 100$  credits;  $\eta_s = (1, 3, 5, 7)$  credits per sample;  $\eta_c = 1.2$  credits per pixel;  $t_{\max} = 18$  s; experiment 4:  $R_0 = 100$  credits;  $\eta_s = 3$  credits per sample;  $\eta_c = (0.5, 1.5, 1.9, 2.6)$  credits per pixel;  $t_{\max} = 18$  s; experiment 5:  $R_0 = 100$  credits;  $\eta_s = 3$  credits per sample;  $\eta_c = 1.2$  credits per pixel;  $t_{\max} = (6, 10, 14, 18)$  s; Extended Data Fig. 2). The four trial types were inter-mixed and the location of the hidden circle was chosen randomly for each trial.

In all of the experiments, task instructions were delivered at the beginning of the session using an automated script. This script presented the rules of the game and included a practice trial with step-by-step instructions popping up on the screen. The experimenter proceeded to the rest of the testing if participants demonstrated sufficient understanding of the task (no participant was excluded for not understanding the task). All participants also completed a debriefing questionnaire at the end of the experimental session to ensure they understood the task properly.

**Quantifying information-sampling efficiency.** As illustrated in Fig. 1c, information sampling efficiency was quantified as the rate at which the expected error decreased over successive samples. On average, this relationship was exponential (Extended Data Fig. 4). The value of  $\alpha$  was estimated by fitting the following relationship to individual datasets separately:

$$\begin{aligned} \hat{E}E_{(n,1)} &= \frac{\sum_{i=1}^{96} EE_{(i)}}{96} \\ \hat{E}E_{(n,s)} &= (\hat{E}E_{(n,1)} - \hat{E}E_{\infty}) \times (1 - \alpha_n)^{s-1} + \hat{E}E_{\infty} \\ 0 < \alpha < 1 \text{ and } \hat{E}E_{\infty} > 0 \end{aligned} \quad (2)$$

where  $n$  is the trial number and  $s$  is the serial position of the sample within the trial (the 0th sample was the one displayed on the screen at the beginning of the trial, before participants touched the screen; Fig. 1a). This simple model was fitted using a least-mean-squared error procedure, implemented in MATLAB (MathWorks version 2018a) with the function `fmincon`. For each participant,

parameter estimation yielded one  $\alpha$  per trial and one positive asymptote  $\hat{E}E_{\infty}$  for all trials. The former captured how much individual observations reduced uncertainty within a given trial (higher  $\alpha$  means more efficient sampling, that is, sharper reduction of the expected error). The latter captures the asymptotic limit of information gathering for a given participant.

**Computational model of sampling speed, efficiency and extent.** From a neuroeconomic perspective, behaving optimally means adopting the course of action—parameterized here as the combination of  $(ISI, \alpha, s)$ —that maximizes the expected value of the final response (Fig. 4a). This variable provides a predictive estimate of the reward expected to arise from placing the blue disk. Numerically, it is calculated as:

$$\begin{aligned} EV_0 &= R_0 - \eta_e \times EE_0 \\ EV_s( ISI, \alpha, t_{max} ) &= EV_{s-1} + p(s| ISI, t_{max}) \\ &\quad \times [\eta_e \times (1 - \alpha) \times (EE_{s-1} - \hat{E}E_{\infty}) - \eta_s] \end{aligned} \tag{3}$$

(in words, expected value of sample = previous expected value + probability of acquiring the sample given the current time  $\times$  [expected information benefit – sampling cost]), where the probability of acquiring a sample is 1 during the time allocated to the search and null otherwise:

$$\begin{cases} p(s| ISI, t_{max}) = 1 \text{ if } s \times ISI \leq t_{max} \\ p(s| ISI, t_{max}) = 0 \text{ if } s \times ISI > t_{max} \end{cases} \tag{4}$$

Note that the interaction between economic variables and time pressure is built in the architecture of the model. The time allocated to the search ( $t_{max}$ ) influences the number of acquirable samples for a given sampling rate, while economic variables ( $R_0, \eta_e$ , and  $\eta_c$ ) influence the magnitude of the expected value at each step. Thus, the two interact in a multiplicative manner. For example, manipulating the time pressure when errors are strongly penalized (that is, every sample induces a large change in the expected value) has a greater influence on utility than when errors are weakly penalized (that is, every sample induces a small change in the expected value). Although this type of interaction was not tested here for practical reasons, it could be done in future studies.

The rational expected value model was modified as follows to build the models evaluated in this work. Note that the expected value is replaced by an expected utility because its specification departs from the rational definition:

$$\begin{aligned} EU_0 &= R_0 - \eta_e \times EE_0 \\ EU_s( ISI, \alpha, t_{max} ) &= EU_{s-1} + p(s| ISI, t_{max}) \times [w_e \times \eta_e \times (1 - \alpha) \\ &\quad \times (EE_{s-1} - \hat{E}E_{\infty}) - w_s \times \eta_s^{1+\gamma_s} - \eta_c( ISI, \alpha )] \end{aligned} \tag{5}$$

(in words, expected utility of sample = previous expected utility + probability of acquiring the sample given the current time  $\times$  [expected information benefit – sampling cost – cognitive effort cost]), where  $\gamma$  is a power term introducing a nonlinear transformation of the sampling cost over successive samples and  $\eta_c( ISI, \alpha )$  is a cognitive effort cost function. The information-gathering asymptotic limit,  $\hat{E}E_{\infty}$ , was estimated for each individual by fitting equation (2) beforehand. Thus, the modelling of active information sampling behaviour  $( ISI, \alpha, s )$  took into consideration inter-individual differences in asymptotic information gathering performance.

Various cognitive effort cost functions were evaluated in the paper:

$$\begin{aligned} \eta_c( ISI, \alpha ) &= 0 \quad (\text{no cost}) \\ \eta_c( ISI, \alpha ) &= w_0 + w_{speed} \times \frac{1}{ISI} + w_{\alpha} \times \alpha \quad (\text{linear}) \\ \eta_c( ISI, \alpha ) &= w_0 + w_{speed} \times \frac{1}{ISI^2} + w_{\alpha} \times \alpha^2 \quad (\text{quadratic}) \\ \eta_c( ISI, \alpha ) &= A \times e^{w_0 + w_{speed} \times \frac{1}{ISI} + w_{\alpha} \times \alpha} \quad (\text{exponential}) \\ \eta_c( ISI, \alpha ) &= \frac{A}{1 + e^{w_0 - w_{speed} \times \frac{1}{ISI} - w_{\alpha} \times \alpha}} \quad (\text{sigmoid}) \end{aligned} \tag{6}$$

All models reported in the paper also included a free intercept,  $w_0$  (versions without an intercept are reported in Supplementary Fig. 2). Logistic and exponential cost functions required the addition of an extra free scaling parameter,  $A$ .

For each of the linear, quadratic, exponential and sigmoid classes, three versions of the model were built: (1) only speed penalized ( $w_e = 0$ ); (2) only efficiency penalized ( $w_{speed} = 0$ ); and (3) both speed and efficiency penalized. The sampling cost power term,  $\gamma$ , was only included in the absence of a cognitive effort cost ( $\eta_c( ISI, \alpha ) = 0$ ; model 2) to act as a second reference model and to ask whether a nonlinear utility function could account for the data without the cognitive effort costs. It was never used in combination with a linear, quadratic, exponential or logistic cognitive effort cost function, to prevent over-fitting by overly complex models. An exhaustive description of the free parameters included in each model is provided in Extended Data Fig. 5.

The likelihood function was obtained by applying a softmax function over the three-dimensional space of expected utility (the expected utility is a function of  $ISI, \alpha$  and  $s$ ) for a given task environment (a combination of  $R_0, \eta_s, \eta_e$  and  $t_{max}$ ), as follows:

$$p_s(\text{stop} | ISI, \alpha, t_{max}) = \frac{\exp(EU_s( ISI, \alpha, t_{max} ))}{\sum_i \sum_a \sum_{i'}^{\max} \exp(EU_s( i, a, t ))} \tag{7}$$

Model fitting involved finding, for each individual separately, the parameters that minimized the negative log-likelihood of observing the multivariate distribution of the number of samples acquired ( $s$ ; one value per trial),  $ISI$  (averaged across samples within a trial to obtain one value per trial) and sampling efficiency ( $\alpha$ ; one value per trial). Note that sampling speed and efficiency were assumed to be stationary within a trial (that is, one combination of  $(s, ISI, \alpha)$  per trial). Although it is an approximation of actual human behaviour, this assumption was necessary to simplify the framework. Parameter optimization was carried out in MATLAB (MathWorks version 2018a) using Bayesian adaptive direct search<sup>31</sup>, which was chosen for its high performance with non-smooth cost functions. Model fits were compared using BIC, which quantifies the goodness of fit while penalizing models for the number of free parameters, to avoid over-fitting.

**Statistical analysis.** Data handling and statistical analysis were performed in MATLAB (MathWorks version 2018a). Mixed-effect models with maximal random structure were used for statistical analysis of behavioural measures. When relevant, the trial index was included as a random effect to control for potential learning effects throughout the task (see Supplementary Fig. 4 for a visualization of these effects). Extended details (link function, data transformation, model specification, parameter estimates and statistics) are provided in Supplementary Tables 1–15. Robust multiple linear regression was used to investigate the relationship between fatigue development (block 8 minus baseline) and the parameters of the winning cognitive effort cost function in experiment 1b ( $w_0, w_{speed}$  and  $w_{\alpha}$ ) while controlling for the experiment duration. This method uses an iteratively re-weighted least-squares procedure to limit the contribution of potential outliers to the linear fit. All statistical tests were two sided. No a priori hypotheses/predictions were altered after the data were analysed or during the course of writing/revising the paper.

**Reporting Summary.** Further information on research design is available in the Nature Research Reporting Summary linked to this article.

**Data availability**

Anonymized participant data have been deposited on the Open Science Framework platform and can be found at <https://osf.io/25wkh/>.

**Code availability**

Code for replicating the main results reported in the manuscript has been deposited on the Open Science Framework platform and can be found at <https://osf.io/25wkh/>. Additional analysis codes are available on request from the corresponding authors.

Received: 16 June 2020; Accepted: 14 April 2021; Published online: 27 May 2021

**References**

- Clark, L., Robbins, T. W., Ersche, K. D. & Sahakian, B. J. Reflection impulsivity in current and former substance users. *Biol. Psychiatry* **60**, 515–522 (2006).
- Battaglia, P. W. & Schrater, P. R. Humans trade off viewing time and movement duration to improve visuomotor accuracy in a fast reaching task. *J. Neurosci.* **27**, 6984–6994 (2007).
- Gottlieb, J., Oudeyer, P. Y., Lopes, M. & Baranes, A. Information-seeking, curiosity, and attention: computational and neural mechanisms. *Trends Cogn. Sci.* **17**, 585–593 (2013).
- Averbeck, B. B. Theory of choice in bandit, information sampling and foraging tasks. *PLoS Comput. Biol.* **11**, e1004164 (2015).
- Juni, M. Z., Gureckis, T. M. & Maloney, L. T. ‘Information sampling behavior with explicit sampling costs’: correction to Juni, Gureckis, and Maloney (2015). *Decision* **3**, 168 (2016).
- Hauser, T. U., Moutoussis, M., Dayan, P. & Dolan, R. J. Increased decision thresholds trigger extended information gathering across the compulsivity spectrum. *Transl. Psychiatry* **7**, 1296 (2017).
- Savage, L. J. *The Foundations of Statistics* (Courier Corporation, 1972).
- Tversky, A. & Kahneman, D. Advances in prospect theory: cumulative representation of uncertainty. *J. Risk Uncertain.* **5**, 297–323 (1992).
- Von Neumann, J., Morgenstern, O. & Kuhn, H. W. *Theory of Games and Economic Behavior, Commemorative Edition* (Princeton Univ. Press, 2007).
- Johnson, J. G. & Busemeyer, J. R. Decision making under risk and uncertainty. *Wiley Interdiscip. Rev. Cogn. Sci.* **1**, 736–749 (2010).

11. Kahneman, D. & Tversky, A. in *Handbook of the Fundamentals of Financial Decision Making* Vol. 4 99–127 (World Scientific, 2012).
12. Chamberlain, S. R. et al. A neuropsychological comparison of obsessive-compulsive disorder and trichotillomania. *Neuropsychologia* **45**, 654–662 (2007).
13. Furl, N. & Averbeck, B. B. Parietal cortex and insula relate to evidence seeking relevant to reward-related decisions. *J. Neurosci.* **31**, 17572–17582 (2011).
14. Djamshidian, A. et al. Decision making, impulsivity, and addictions: do Parkinson's disease patients jump to conclusions? *Mov. Disord.* **27**, 1137–1145 (2012).
15. Hauser, T. U. et al. Increased decision thresholds enhance information gathering performance in juvenile obsessive-compulsive disorder (OCD). *PLoS Comput. Biol.* **13**, e1005440 (2017).
16. Hauser, T. U., Moutoussis, M., Purg, N., Dayan, P. & Dolan, R. J. Beta-blocker propranolol modulates urgency during sequential information gathering. *J. Neurosci.* **38**, 7170–7178 (2018).
17. Jones, P. R. et al. Efficient visual information sampling develops late in childhood. *J. Exp. Psychol. Gen.* **148**, 1138–1152 (2019).
18. Hertwig, R., Barron, G., Weber, E. U. & Erev, I. Decisions from experience and the effect of rare events in risky choice. *Psychol. Sci.* **15**, 534–539 (2004).
19. Gottlieb, J. & Oudeyer, P. Y. Towards a neuroscience of active sampling and curiosity. *Nat. Rev. Neurosci.* **19**, 758–770 (2018).
20. Bossaerts, P., Yadav, N. & Murawski, C. Uncertainty and computational complexity. *Phil. Trans. R. Soc. B* **374**, 20180138 (2019).
21. Kurzban, R., Duckworth, A., Kable, J. W. & Myers, J. An opportunity cost model of subjective effort and task performance. *Behav. Brain Sci.* **36**, 661–679 (2013).
22. Boureau, Y.-L., Sokol-Hessner, P. & Daw, N. D. Deciding how to decide: self-control and meta-decision making. *Trends Cogn. Sci.* **19**, 700–710 (2015).
23. Shenhav, A., Botvinick, M. M. & Cohen, J. D. The expected value of control: an integrative theory of anterior cingulate cortex function. *Neuron* **79**, 217–240 (2013).
24. Westbrook, A. & Braver, T. S. Cognitive effort: a neuroeconomic approach. *Cogn. Affect. Behav. Neurosci.* **15**, 395–415 (2015).
25. Horan, M., Daddaoua, N. & Gottlieb, J. Parietal neurons encode information sampling based on decision uncertainty. *Nat. Neurosci.* **22**, 1327–1335 (2019).
26. Phillips, L. D. & Edwards, W. Conservatism in a simple probability inference task. *J. Exp. Psychol.* **72**, 346–354 (1966).
27. Tversky, A. & Edwards, W. Information versus reward in binary choices. *J. Exp. Psychol.* **71**, 680–683 (1966).
28. Dixon, M. L. & Christoff, K. The decision to engage cognitive control is driven by expected reward-value: neural and behavioral evidence. *PLoS ONE* **7**, e51637 (2012).
29. Shenhav, A., Botvinick, M. M. & Cohen, J. D. The expected value of control: an integrative theory of anterior cingulate cortex function. *Neuron* **79**, 217–240 (2013).
30. Manohar, S. G. et al. Reward pays the cost of noise reduction in motor and cognitive control. *Curr. Biol.* **25**, 1707–1716 (2015).
31. Acerbi, L. & Ma, W. J. Practical Bayesian optimization for model fitting with Bayesian adaptive direct search. *Adv. Neural Inf. Process. Syst.* **30**, 1836–1846 (2017).
32. Bogacz, R., Wagenmakers, E.-J., Forstmann, B. U. & Nieuwenhuis, S. The neural basis of the speed-accuracy tradeoff. *Trends Neurosci.* **33**, 10–16 (2010).
33. Carpenter, P. A., Just, M. A. & Shell, P. What one intelligence test measures: a theoretical account of the processing in the Raven progressive matrices test. *Psychol. Rev.* **97**, 404–431 (1990).
34. Ang, Y. S., Lockwood, P., Apps, M. A., Muhammed, K. & Husain, M. Distinct subtypes of apathy revealed by the apathy motivation index. *PLoS ONE* **12**, e0169938 (2017).
35. Patton, J. H., Stanford, M. S. & Barratt, E. S. Factor structure of Barratt impulsiveness scale. *J. Clin. Psychol.* **51**, 768–774 (1995).
36. Charnov, E. L. et al. *Optimal Foraging, the Marginal Value Theorem* (Academic Press, 1976).
37. Kolling, N., Behrens, T. E. J., Mars, R. B. & Rushworth, M. F. S. Neural mechanisms of foraging. *Science* **336**, 95–98 (2012).
38. Shenhav, A. et al. Toward a rational and mechanistic account of mental effort. *Annu. Rev. Neurosci.* **40**, 99–124 (2017).
39. Payne, J. W., Payne, J. W., Bettman, J. R. & Johnson, E. J. *The Adaptive Decision Maker* (Cambridge Univ. Press, 1993).
40. Stark, D. P. & Choplin, J. M. A license to deceive: enforcing contractual myths despite consumer psychological realities academic article. *NY Univ. J. Law Bus.* **5**, 617–744 (2009).
41. Otto, A. R. & Daw, N. D. The opportunity cost of time modulates cognitive effort. *Neuropsychologia* **123**, 92–105 (2019).
42. Hasenstaub, A., Otte, S., Callaway, E. & Sejnowski, T. J. Metabolic cost as a unifying principle governing neuronal biophysics. *Proc. Natl Acad. Sci. USA* **107**, 12329–12334 (2010).
43. Kitzbichler, M. G., Henson, R. N. A., Smith, M. L., Nathan, P. J. & Bullmore, E. T. Cognitive effort drives workspace configuration of human brain functional networks. *J. Neurosci.* **31**, 8259–8270 (2011).
44. Bullmore, E. & Sporns, O. The economy of brain network organization. *Nat. Rev. Neurosci.* **13**, 336–349 (2012).
45. Kostal, L. & Kobayashi, R. Optimal decoding and information transmission in Hodgkin-Huxley neurons under metabolic cost constraints. *Biosystems* **136**, 3–10 (2015).
46. Hartmanis, J. & Stearns, R. E. On the computational complexity of algorithms. *Trans. Am. Math. Soc.* **117**, 285–306 (1965).
47. Arora, S. & Barak, B. *Computational Complexity: a Modern Approach* (Cambridge Univ. Press, 2009).
48. Jones, M. & Sugden, R. Positive confirmation bias in the acquisition of information. *Theory Decis.* **50**, 59–99 (2001).
49. Huys, Q. J. M. et al. Bonsai trees in your head: how the Pavlovian system sculpts goal-directed choices by pruning decision trees. *PLoS Comput. Biol.* **8**, e1002410 (2012).
50. Körding, K. P. & Wolpert, D. M. Bayesian decision theory in sensorimotor control. *Trends Cogn. Sci.* **10**, 319–326 (2006).
51. Husain, M. & Roiser, J. P. Neuroscience of apathy and anhedonia: a transdiagnostic approach. *Nat. Rev. Neurosci.* **19**, 470–484 (2018).
52. Fleming, S. M. & Lau, H. C. How to measure metacognition. *Front. Hum. Neurosci.* **8**, 443 (2014).
53. Vaghi, M. M. et al. Compulsivity reveals a novel dissociation between action and confidence. *Neuron* **96**, 348–354.e4 (2017).
54. Silvetti, M., Vassena, E., Abrahamse, E. & Verguts, T. Dorsal anterior cingulate-brainstem ensemble as a reinforcement meta-learner. *PLoS Comput. Biol.* **14**, e1006370 (2018).
55. Bonneville, V., Manohar, S., Behrens, T. & Husain, M. Individual differences in premotor brain systems underlie behavioral apathy. *Cereb. Cortex* **26**, 807–819 (2016).
56. Lockwood, P. L. et al. Prosocial apathy for helping others when effort is required. *Nat. Hum. Behav.* **1**, 0131 (2017).
57. Brainard, D. H. The psychophysics toolbox. *Spat. Vis.* **10**, 433–436 (1997).
58. Kleiner, M. et al. What's new in Psychtoolbox-3? *Perception* **36**, 1–16 (2007).
59. Chong, T. T. et al. Neurocomputational mechanisms underlying subjective valuation of effort costs. *PLoS Biol.* **15**, e1002598 (2017).
60. Le Heron, C. et al. Dysfunctional effort-based decision-making underlies apathy in genetic cerebral small vessel disease. *Brain* **141**, 3193–3210 (2018).
61. Le Heron, C. et al. Distinct effects of apathy and dopamine on effort-based decision-making in Parkinson's disease. *Brain* **141**, 1455–1469 (2018).
62. Beck, A. T., Ward, C. H., Mendelson, M., Mock, J. & Erbaugh, J. An inventory for measuring depression. *Arch. Gen. Psychiatry* **4**, 561–571 (1961).
63. Buhr, K. & Dugas, M. The Intolerance of Uncertainty Scale: psychometric properties of the English version. *Behav. Res. Ther.* **40**, 931–945 (2002).

### Acknowledgements

We thank L. Acerbi for help designing an optimal search algorithm (infoMax) and M. Serrano Bonilla for help with figure design. We also thank all of the members of the Cognitive Neurology Research Group for assistance as experimental confederates. This work was supported by the Wellcome Trust (206330/Z/17/Z). P.P. and M.H. were funded by the Wellcome Trust (206330/Z/17/Z). B.A. was funded by a Rhodes Scholarship. S.G.M. was funded by an MRC Clinician Scientist Fellowship (MR/P00878/X). The funders had no role in study design, data collection and analysis, decision to publish or preparation of the manuscript.

### Author contributions

P.P., B.A. and M.H. designed the study. P.P. and B.A. collected the data. P.P., B.A. and S.G.M. analysed the data. P.P. and M.H. wrote the paper.

### Competing interests

The authors declare no competing interests.

### Additional information

**Extended data** is available for this paper at <https://doi.org/10.1038/s41562-021-01116-6>.

**Supplementary information** The online version contains supplementary material available at <https://doi.org/10.1038/s41562-021-01116-6>.

**Correspondence and requests for materials** should be addressed to P.P. or M.H.

**Peer review information** *Nature Human Behaviour* thanks Jacqueline Gottlieb and the other, anonymous, reviewer(s) for their contribution to the peer review of this work.

**Reprints and permissions information** is available at [www.nature.com/reprints](http://www.nature.com/reprints).

**Publisher's note** Springer Nature remains neutral with regard to jurisdictional claims in published maps and institutional affiliations.

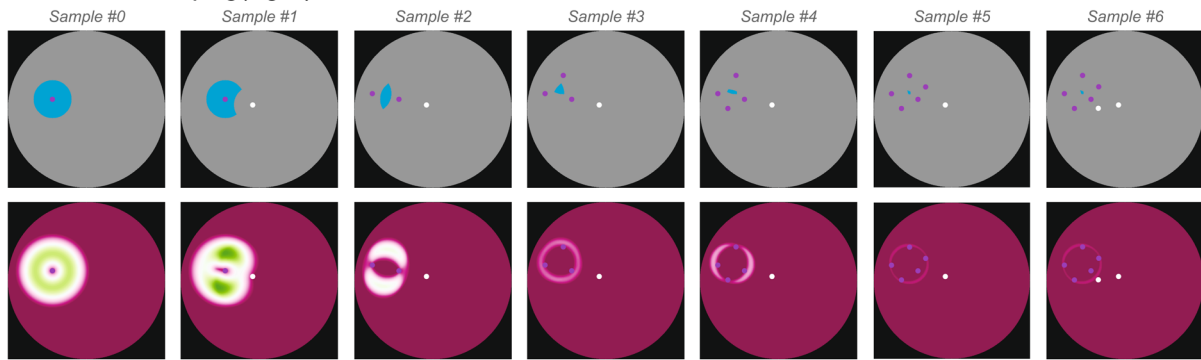
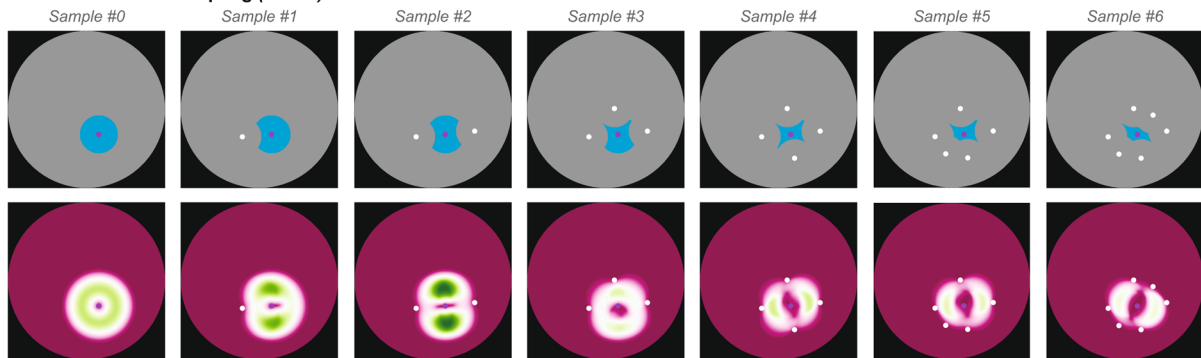
© The Author(s), under exclusive licence to Springer Nature Limited 2021

	Exp. 1	Exp. 2	Exp. 3	Exp. 4	Exp. 5
<b>Age</b>	24.5 (3.8)	24.9 (3.8)	25.7 (5.2)	26.1 (4.0)	23.7 (2.6)
<b>Sex</b>	24F/24M	10F/10M	10F/10M	10F/10M	10F/9M
<b>YOE</b>	18.4 (3.2)	18.3 (4.0)	17.1 (3.2)	17.8 (2.1)	17.4 (1.3)
<b>Raven's matrices</b>	8.7 (2.4)	7.5 (2.6)	8.7 (2.0)	7.5 (1.8)	7.6 (2.9)
<b>BDI total score</b>	7.3 (5.5)	7.1 (5.2)	5.4 (5.0)	7.2 (6.5)	7.6 (7.8)
<b>AMI total score</b>	1.4 (0.5)	1.3 (0.4)	1.3 (0.4)	1.3 (0.3)	1.1 (0.4)
<b>BIS total score</b>	62.3 (9.8)	64.8 (10.7)	58.7 (9.1)	63.0 (13.0)	62.6 (13.6)
<b>IUS total score</b>	60.5 (17.3)	60.8 (21.9)	61.7 (20.0)	59.9 (13.0)	66.4 (24.4)
<b>Active task duration (min)</b>	47.3 (1.3)	51.5 (4.1)	50.0 (2.2)	50.4 (2.3)	42.2 (3.0)
<b>Passive task duration (min)</b>	41.7 (2.0)	-	-	-	-

**Extended Data Fig. 1 | Demographic and questionnaire measures.** The table shows group means with standard deviation in parenthesis. F: Female; M: Male; YOE: years of education (since kindergarten); BDI: Beck Depression Inventory-II; AMI: Apathy Motivation Index; BIS-11: Barratt Impulsiveness Scale-11; IUS: Intolerance of Uncertainty Scale.

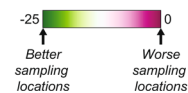
	$R_0$	$\eta_s$	$\eta_e$	$t_{max}$	$n$ trials
<b>Exp. 1b</b>	125	1			24
	100	1			24
	125	5	1.2	18 secs	24
	100	5			24
<b>Exp. 2</b>	50				24
	75	3	1.2	18 secs	24
	100				24
	125				24
<b>Exp. 3</b>		1			24
		3			24
	100	5	1.2	18 secs	24
		7			24
<b>Exp. 4</b>			0.5		24
			1.2		24
	100	3	1.9	18 secs	24
			2.6		24
<b>Exp. 5</b>				6 secs	24
				10 secs	24
	100	3	1.2	14 secs	24
				18 secs	24

**Extended Data Fig. 2 | Experimental design.** All experiments included four types of trial (24 repetitions per trial type; 96 trials in total). The cost-benefit and temporal structure of these trial types is depicted here.  $R_0$ : initial credit;  $\eta_s$ : sampling cost;  $\eta_e$ : error cost;  $t_{max}$ : time allocated to the sampling phase.

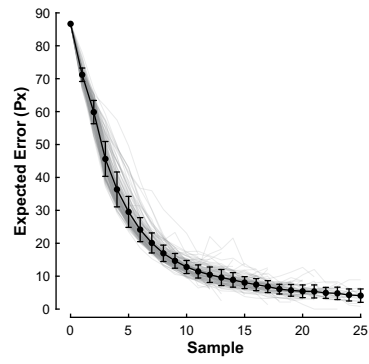
a. Efficient information sampling (*High  $\alpha$* )b. Inefficient information sampling (*Low  $\alpha$* )

Top row : Posterior belief

Bottom row : Expected change in EE



**Extended Data Fig. 3 | A visual illustration of efficient versus inefficient sampling.** A map of the posterior belief (top row) and of the expected change in expected error (EE) (bottom row) is plotted for the two example trials plotted in Fig. 1c (panel a: High  $\alpha$  trial; panel b: Low  $\alpha$  trial). The posterior belief map represents (in blue) all pixels that may be the centre of the hidden circle given the information on the screen (grey: search space; purple dots: observations inside the hidden circle; white dots: observations outside the hidden circle). The smaller this area, the lower the overall uncertainty (EE). For each sample, the associated map represents the change in EE expected to occur for every possible candidate sampling location. An efficient sampler systematically samples where the expected  $\Delta EE$  is the lowest. a. During efficient sampling, the area covered by the posterior belief decays because the participant samples where the expected  $\Delta EE$  is the lowest. b. By contrast, when sampling is inefficient, the area covered by the posterior belief decays less sharply because the participant does not sample where the expected  $\Delta EE$  is the lowest.

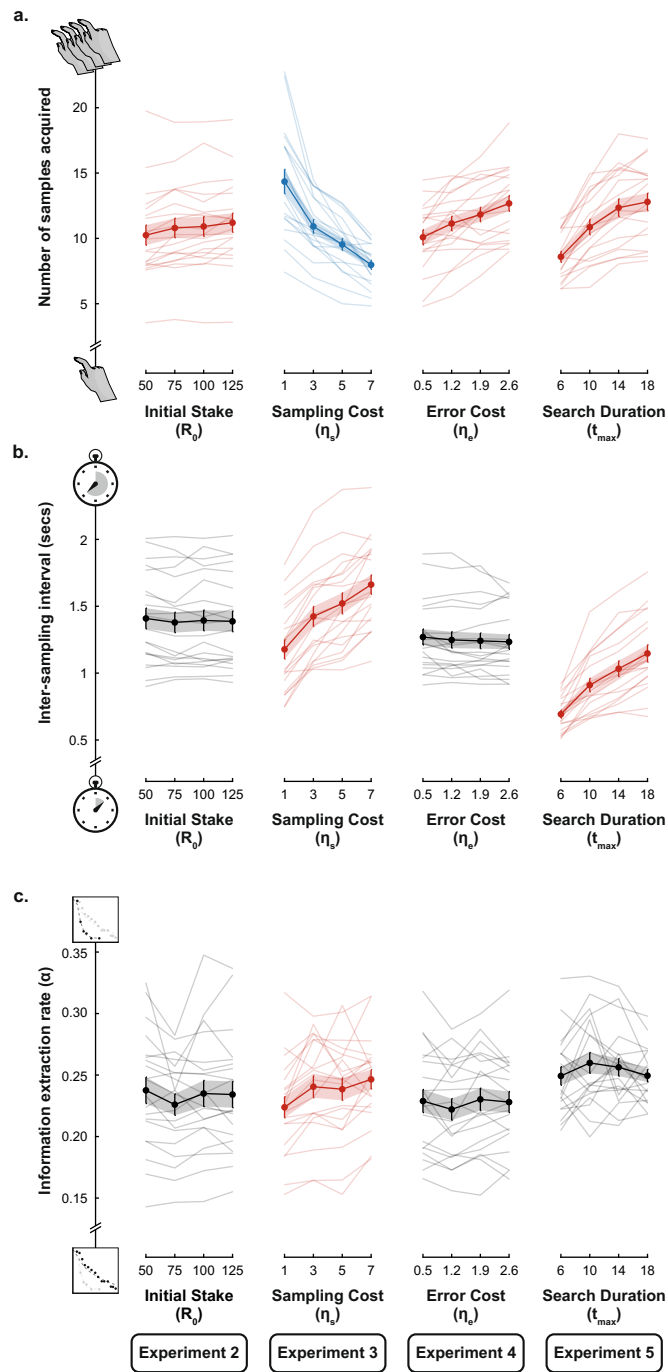


**Extended Data Fig. 4 |** On average, the expected error decreases exponentially over successive samples. Grey lines represent, for each participant ( $n = 127$  across all five experiments), the average Expected Error as a function of sample index. The black line shows the average across all participants ( $\pm$  s.d.).

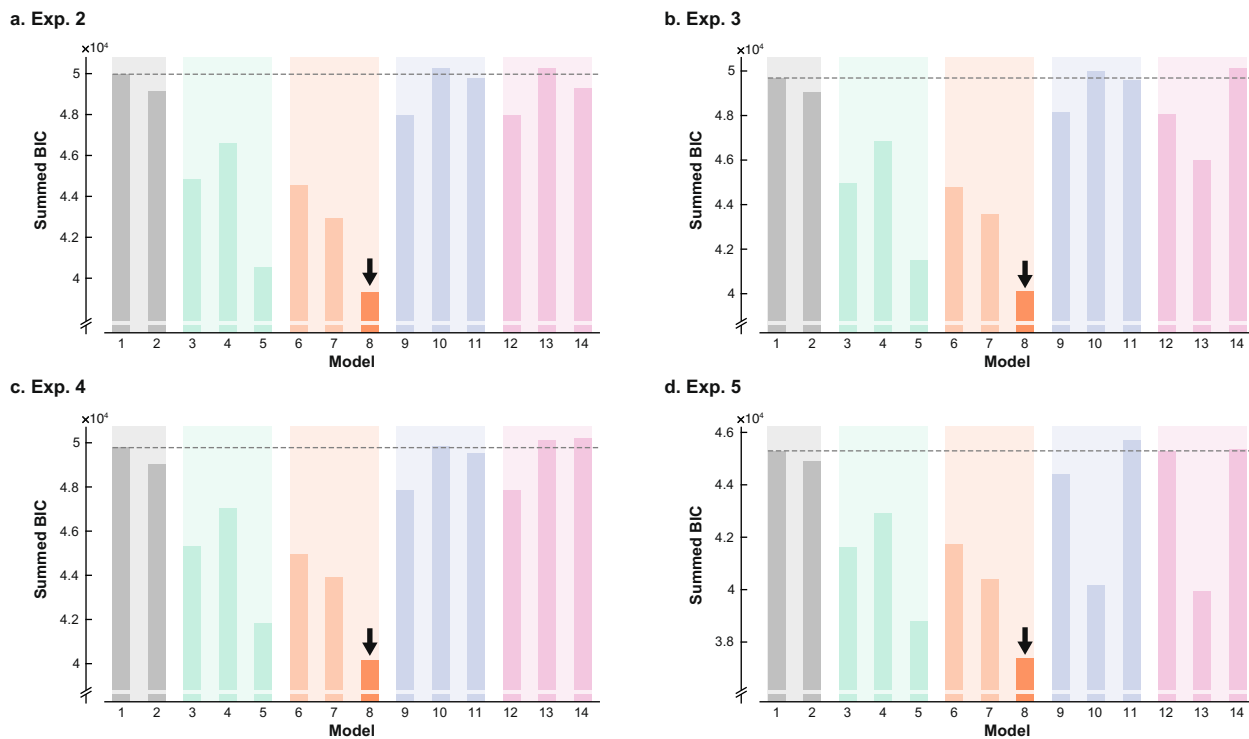


	$w_e$	$w_s$	$\gamma$	$w_0$	$w_{speed}$	$w_\alpha$	$A$	<i>n free parameters</i>
Model 1	✓	✓	x	x	x	x	x	2
Model 2	✓	✓	✓	x	x	x	x	3
Model 3	✓	✓	x	✓	✓	x	x	4
Model 4	✓	✓	x	✓	x	✓	x	4
Model 5	✓	✓	x	✓	✓	✓	x	5
Model 6	✓	✓	x	✓	✓	x	x	4
Model 7	✓	✓	x	✓	x	✓	x	4
<b>Model 8*</b>	✓	✓	x	✓	✓	✓	x	5
Model 9	✓	✓	x	✓	✓	x	✓	5
Model 10	✓	✓	x	✓	x	✓	✓	5
Model 11	✓	✓	x	✓	✓	✓	✓	6
Model 12	✓	✓	x	✓	✓	x	✓	5
Model 13	✓	✓	x	✓	x	✓	✓	5
Model 14	✓	✓	x	✓	✓	✓	✓	6
Model 15	✓	✓	x	x	✓	x	x	3
Model 16	✓	✓	x	x	x	✓	x	3
Model 17	✓	✓	x	x	✓	✓	x	4
Model 18	✓	✓	x	x	✓	x	x	3
Model 19	✓	✓	x	x	x	✓	x	3
Model 20	✓	✓	x	x	✓	✓	x	4
Model 21	✓	✓	x	x	✓	x	✓	4
Model 22	✓	✓	x	x	x	✓	✓	4
Model 23	✓	✓	x	x	✓	✓	✓	5
Model 24	✓	✓	x	x	✓	x	✓	4
Model 25	✓	✓	x	x	x	✓	✓	4
Model 26	✓	✓	x	x	✓	✓	✓	5

**Extended Data Fig. 5 | Free parameters included in our models of speed, efficiency and extent of active information sampling.** Models were defined using the equation reported in the Methods. Tick: parameter included in the model and estimated through the fitting procedure; Cross: parameter not included in the model (effectively set to zero). \*: Winning model (Model comparison in Fig. 5, Extended Data Fig. 7& Supplementary Fig. 2).



**Extended Data Fig. 6 | Economic and time constraints influence the extent, speed and efficiency of active information sampling.** a. Individuals sampled more with large initial reward reserves (Exp. 2,  $n = 20$ ), when acquiring data was cheap (Exp. 3,  $n = 20$ ), when final error was strongly penalised (Exp. 4,  $n = 20$ ), and when they had time to search (Exp. 5,  $n = 19$ ). Hand icon adapted from Freepik: macrovector. b-c. The initial credit and severity of error discounting did not influence how quickly or efficiently participants resolved localisation uncertainty (Exps. 2 & 4). Players sampled slower but more efficiently when acquiring data was more expensive (Exp. 3). By contrast, they speeded up but maintained a high level of efficiency (indexed by information extraction rate) under tighter time pressure (Exp. 5). Points and error bars show group mean  $\pm$  s.e.m. Lines show condition averages for each participant. Positive/negative main effect of the experimental variable manipulated is shown in red/blue. Full statistical details are reported in Supplementary Tables 3-5.



**Extended Data Fig. 7 | Model comparison from Experiments 2-5.** The same models as in Fig. 5 are compared here. Model 1 and 2 included no cognitive effort cost (Model 1: rational specification; Model 2: nonlinear utility function; in grey) and were used as a reference. The other 12 models included a cognitive effort cost specified in terms of either speed (Models 3, 6, 9, 12), efficiency (Models 4, 7, 10, 13) or both (Models 5, 8, 11, 14). They differed with respect to the shape of the cost function (green: linear; orange: quadratic; blue: exponential; pink: sigmoid). Across all four experiments, participants' choices of sampling speed, efficiency and extent were best explained by a model penalising both speed and efficiency with a quadratic cost function (Model 8, lowest Bayesian Information Criterion, BIC).

## Reporting Summary

Nature Research wishes to improve the reproducibility of the work that we publish. This form provides structure for consistency and transparency in reporting. For further information on Nature Research policies, see our [Editorial Policies](#) and the [Editorial Policy Checklist](#).

### Statistics

For all statistical analyses, confirm that the following items are present in the figure legend, table legend, main text, or Methods section.

n/a Confirmed

- |                                     |                                     |  |
|-------------------------------------|-------------------------------------|--|
| <input type="checkbox"/>            | <input checked="" type="checkbox"/> | The exact sample size ( $n$ ) for each experimental group/condition, given as a discrete number and unit of measurement  |
| <input type="checkbox"/>            | <input checked="" type="checkbox"/> | A statement on whether measurements were taken from distinct samples or whether the same sample was measured repeatedly  |
| <input type="checkbox"/>            | <input checked="" type="checkbox"/> | The statistical test(s) used AND whether they are one- or two-sided<br><i>Only common tests should be described solely by name; describe more complex techniques in the Methods section.</i>   |
| <input type="checkbox"/>            | <input checked="" type="checkbox"/> | A description of all covariates tested   |
| <input type="checkbox"/>            | <input checked="" type="checkbox"/> | A description of any assumptions or corrections, such as tests of normality and adjustment for multiple comparisons  |
| <input type="checkbox"/>            | <input checked="" type="checkbox"/> | A full description of the statistical parameters including central tendency (e.g. means) or other basic estimates (e.g. regression coefficient) AND variation (e.g. standard deviation) or associated estimates of uncertainty (e.g. confidence intervals) |
| <input type="checkbox"/>            | <input checked="" type="checkbox"/> | For null hypothesis testing, the test statistic (e.g. $F$ , $t$ , $r$ ) with confidence intervals, effect sizes, degrees of freedom and $P$ value noted<br><i>Give <math>P</math> values as exact values whenever suitable.</i>                            |
| <input checked="" type="checkbox"/> | <input type="checkbox"/>            | For Bayesian analysis, information on the choice of priors and Markov chain Monte Carlo settings   |
| <input type="checkbox"/>            | <input checked="" type="checkbox"/> | For hierarchical and complex designs, identification of the appropriate level for tests and full reporting of outcomes   |
| <input checked="" type="checkbox"/> | <input type="checkbox"/>            | Estimates of effect sizes (e.g. Cohen's $d$ , Pearson's $r$ ), indicating how they were calculated   |

*Our web collection on [statistics for biologists](#) contains articles on many of the points above.*

### Software and code

Policy information about [availability of computer code](#)

Data collection: MATLAB version 2018a (MathWorks; <https://uk.mathworks.com>)

Data analysis: Custom code written in MATLAB version 2018a  
For the drift-diffusion model: HDDM 0.6.0 in Python 2.7

For manuscripts utilizing custom algorithms or software that are central to the research but not yet described in published literature, software must be made available to editors and reviewers. We strongly encourage code deposition in a community repository (e.g. GitHub). See the Nature Research [guidelines for submitting code & software](#) for further information.

### Data

Policy information about [availability of data](#)

All manuscripts must include a [data availability statement](#). This statement should provide the following information, where applicable:

- Accession codes, unique identifiers, or web links for publicly available datasets
- A list of figures that have associated raw data
- A description of any restrictions on data availability

All experimental/analysis code and data related to this paper are available from the corresponding author upon reasonable request.

## Field-specific reporting

Please select the one below that is the best fit for your research. If you are not sure, read the appropriate sections before making your selection.

Life sciences  Behavioural & social sciences  Ecological, evolutionary & environmental sciences

For a reference copy of the document with all sections, see [nature.com/documents/nr-reporting-summary-flat.pdf](https://www.nature.com/documents/nr-reporting-summary-flat.pdf)

## Behavioural & social sciences study design

All studies must disclose on these points even when the disclosure is negative.

Study description	The study uses a novel active information sampling task, as well as a passive counterpart. Questionnaire data were also collected. All data are quantitative.
Research sample	Total n = 127 (Exp. 1: n=48, Exps. 2-4: n=20 each, Exp. 5: n=19) Mean age: 24.9 years (SD: 3.9) Gender: 64 females (Exp. 1: 24F/24M, Exps. 2-4: 10F/10M, Exp 5: 10F/9M)  Participants were undergraduates, postgraduates and young professionals, recruited via online study advertisement (Oxford Psychology Research participant recruitment scheme website). Exclusion criteria included personal history of psychiatric or neurological condition.  A sample of young healthy adults was used here because the objective of the study was to characterize normal active information sampling behaviour in the absence of neurological or psychiatric condition.
Sampling strategy	In Exp. 1, prospective volunteers were selected based on their AMI total score (filled online) to ensure a wide range of motivation levels. In each gender sub-group, 12 participants had a score above 1.33, and 12 participants had a score below 1.33.  No sample-size calculation was performed. Sample size was determined a priori based on previous studies with similar objectives.
Data collection	All tasks were presented on a 17-inch touchscreen PC using MATLAB version 2018a and Psychtoolbox version 3. Participants sat in a quiet testing room, within reaching distance of the screen (about 50 cm). Questionnaire data were collected on an iPad tablet, using QUALTRICS.  Recruitment and data collection were carried out by Pierre Petitet and Bahaaeddin Attaallah. An experimenter (sitting about 2-3 meters behind the participants) was present in the room at all time during behavioural testing. Their role was to explain the task at the beginning of the session (using an automated instruction script), and check that participants were engaged in the task throughout the session. They did not provide strategy advices when participants asked.  Researchers were not blind to the experimental condition or study hypothesis, but their influence on performance was abolished by the use of automated, computerised testing procedures.
Timing	Exp. 1: Oct 2018-Dec 2018 Exps. 2-4: July 2019 - September 2019 Exp. 5: Feb 2020
Data exclusions	No data were excluded from the analyses.
Non-participation	No participant dropped out after inclusion.
Randomization	Participants were allocated into experimental groups randomly.

## Reporting for specific materials, systems and methods

We require information from authors about some types of materials, experimental systems and methods used in many studies. Here, indicate whether each material, system or method listed is relevant to your study. If you are not sure if a list item applies to your research, read the appropriate section before selecting a response.

## Materials &amp; experimental systems

n/a	Involvement
<input checked="" type="checkbox"/>	<input type="checkbox"/> Antibodies
<input checked="" type="checkbox"/>	<input type="checkbox"/> Eukaryotic cell lines
<input checked="" type="checkbox"/>	<input type="checkbox"/> Palaeontology and archaeology
<input checked="" type="checkbox"/>	<input type="checkbox"/> Animals and other organisms
<input type="checkbox"/>	<input checked="" type="checkbox"/> Human research participants
<input checked="" type="checkbox"/>	<input type="checkbox"/> Clinical data
<input checked="" type="checkbox"/>	<input type="checkbox"/> Dual use research of concern

## Methods

n/a	Involvement
<input checked="" type="checkbox"/>	<input type="checkbox"/> ChIP-seq
<input checked="" type="checkbox"/>	<input type="checkbox"/> Flow cytometry
<input checked="" type="checkbox"/>	<input type="checkbox"/> MRI-based neuroimaging

## Human research participants

Policy information about [studies involving human research participants](#)

Population characteristics	See above
Recruitment	Participants were recruited via online advertisement. There was a large diversity of professions (or university subjects studied) and nationalities. Like in most experimental psychology studies, most participants were educated (18 years of education on average, s.d.: 3 years). It is therefore possible that the participants we tested performed slightly better than the general population. Nevertheless, we show evidence that performance did not reach ceiling (see Exp. 5 vs. other Exps.).
Ethics oversight	University of Oxford (IRAS ID: 248379, Ethics Approval Reference: 18/SC/0448)

Note that full information on the approval of the study protocol must also be provided in the manuscript.